Investigating Therapeutic Strategies for Treatment of Osteoarthritis in the Knee Joint

By
Sona Rathod

A thesis submitted to Johns Hopkins University in conformity with the requirements for the degree of Master of Science in Engineering

Johns Hopkins University
Baltimore, Maryland
May, 2016

Abstract:

Osteoarthritis (OA) is one of the most common chronic musculoskeletal diseases of the joints and is characterized by degradation of the articular cartilage as well as hypertrophy of the bone. This leads the clinical symptoms of pain, joint stiffness, loss of mobility, and functional impairment. OA affects 33.6% of those 65 years of age and older in the United States [1]. In addition to effecting older populations, OA is also prevalent in young populations as a resultant of injuries and is termed post-traumatic OA. Current treatments of OA include non-steroidal anti-inflammatory drugs, corticosteroid injections, and hyaluronic acid injections. These therapies are targeted towards pain relief and have little to no disease-modifying activity. The following work explores three different therapeutic methods that seek to modify the disease state of OA: 1) Clearance of senescent cells (SCs) by senolytic compounds, 2) Urinary bladder matrix biomaterial injections, and 3) Hyaluronic Acid Binding Peptide (HApep)-polymer system injections.

The first therapy focuses on cellular senescence, which are known to be associated with age-related disorders such as OA. This work further explores the relationship between SC and OA and how eliminating SCs can reverse OA-related aging of the joint. It was found that SC negatively affects the chondrogenic potential of stems cells and that senescent chondrocytes can effect matrix production of healthy chondrocyte populations. Furthermore, it was found that the selective clearance of SC with Nutlin-3a senolytic increased cartilage matrix formation and reduced symptomatic pain in post-traumatic OA mouse model. The second therapy that was explored involved injection of UBM, which contains many biofactors and proteins that can encourage regeneration, into the intra-articular space. Results showed improvement in pain outcomes and also decreased amount of cartilage lesions and proteoglycan loss. Lastly, the injection of a HApep-polymer system was evaluated with the intention of increasing the retention of HA into the joint and improving the efficacy of current HA treatments and it was found that this also decreases cartilage degradation and improved pain outcomes. The three therapies presented in this thesis represent viable strategies for development of disease-modifying treatments for OA.

Thesis Committee:

Jennifer Elisseeff, Ph.D (primary advisor, reader)
Professor, Biomedical Engineering
Director, Translational Tissue Engineering Center
Johns Hopkins University

Kevin Yarema, Ph.D (reader)
Professor, Biomedical Engineering
Johns Hopkins University

Hai-Quan Mao (reader)
Professor, Biomedical Engineering
Johns Hopkins University

Acknowledgements:

I want to thank Dr. Jennifer Elisseeff for all her guidance in research, industry outlook, and the field of biomedical engineering. It was a great honor to be able to work with her and learn about collaborations between start-ups and academia. The work presented in this thesis would not have been possible without the hardworking members of the ortho group in the Elisseeff Lab: Chaekyu Kim, Ok Hee Jeon, and Heather Jacobs as well as the team at Unity Biotechnology in San Francisco, CA for their collaboration with the senescence project. I learned a lot from each of these people, and truly appreciate all their guidance. I would also like to thank Dr. Kevin Yarema and Dr. Hai-Quan Mao for taking the time to read this thesis and provide feedback.

During the past two years at Hopkins I have made some amazing friends that have inspired and challenged me to always be better than my former self and I am incredibly grateful for this. Last but not least, I would like to thank my family and fiancé all of whom have provided continuous support. My parents came from to the US from India with practically nothing, and now have built a strong future for both my sister and I with their encouragement, love, and faith and have thus been a constant source of my determination.

Table of Contents:

List of Tables:

Table 1. List of mouse primer sequences used for gene expression in RT-PCR analysis

Gene *(Mouse)*	**Forward Sequence 5'-3'**	**Reverse Sequence 5'-3'**
$p16^{INK4a}$	AATCTCCGCGAGGAAAGC	GTCTGCAGCGGACTCCATS
MMP3	TTCTGGGCTATACGAGGGCA	CTTCTTCACGGTTGCAGGGA
IL-6	GCTACCAAACTGGATATAATCAGGA	CCAGGTAGCTATGGTACTCCAGAA
MMP13	GGAGCCCTGATGTTTCCCAT	GTCTTCATCGCCTGGACCATA
IL-1β	GTATGGGCTGGACTGTTTC	GCTGTCTGCTCATTCACG
SOX-9	ACCCACAGCTCCCCTGAAG	CTCACCTTCAGTGGCAAGAGC
COL II	CCTCCGTCTACTGTCCACTGA	ATTGGAGCCCTGGATGAGCA
Aggrecan	CGTTGCAGACCAGGAGCAAT	CGGTCATGAAAGTGGCGGTA
β-actin	CAACCGTGAAAAGATGACCC	GTAGATGGGCACAGTGTGGG

Table 2. List of human primer sequences used for gene expression in RT-PCR analysis

Gene *(Human)*	**Forward Sequence 5'-3'**	**Reverse Sequence 5'-3'**
ADAMTS5	GAGGCCAAAAATGGCTATCA	GGCAGGACACCTGCAATTT
NF-kb	AACAGAGAGGATTTCGTT TCC G	TTTGACCTGAGGGTAAGACTT CT
TNF-alpha	CCTCTCTCTAATCAGCCCTCT G	GAGGACCTGGGAGTAGATGAG
$p16^{INK4a}$	AGCTGGAATTACACAGCTGC	GGACTGGCTTGCAATCTTGT
$p21^{Waf1}$	ATTCCATAGGCGTGGGACCT	TCCTGGGCATTTCGGTCAC
MMP3	CACTCACAGACCTGACTCGG	GAGTCAGGGGGAGGTCCATA
IL-6	CCCCTGACCCAACCACAAAT	ATTTGCCGAAGAGCCCTCAG
P53	CCCAAGCAATGGATGATTTGA	GGCATTCTGGGAGCTTCATCT
MMP13	TGGTCCAGGAGATGAAGACC	TCCTCGGAGACTGGTAATGG
IL-1β	GGACAAGCTGAGGAAGATGC	TCGTTATCCCATGTGTCGAA
SOX-9	GCATGAGCGAGGTGCACTC	TCTCGCTTCAGGTCAGCCTTG
COL II	CGCCGCTGTCCTTCGGTGTC	AGGGCTCCGGCTTCCACACAT
Aggrecan	TGGGAACCAGCCTATACCCCAG	CAGTTGCAGAAGGGCCTTCTGTAC
β-actin	GCTCCTCCTGAGCGCAAGTAC	GGACTCGTCATACTCCTGCTTGC

Table 3. List of rat primer sequences used for gene expression in RT-PCR analysis

Gene *(Rat)*	**Forward Sequence 5'-3'**	**Reverse Sequence 5'-3'**
$p16^{INK4a}$	CGTGCGGTATTTGCGGTATC	GCGTGCTTGAGCAGAAGTTA
IL-6	GACTTCCAGCCAGTTGCCTT	AAGTCTCCTCTCCGGACTTGT
IL-1β	TGACTTCACCATGGAACCCG	GGAGACTGCCCATTCTCGAC
IL-6	CCCCTGACCCAACCACAAAT	ATTTGCCGAAGAGCCCTCAG
MMP13	TGTGTGACAGGAGCTAAGGC	ACTGTCCAGTTCGCACAGTC
COL II	GCCAGGATGCCCGAAAATTA	AGGAGGTCCTTTAGGTCCTATG
Aggrecan	GCGATGCCACCTTGGAAATC	GCCATGCATCACTTCACACC
MMP3	TTTGGCCGTCTCTTCCATCC	GCATCGATCTTCTGGACGGT

List of Figures:

List of Abbreviations:

Osteoarthritis (OA)

Post-traumatic OA (PTOA)

senescent associated secretory phenotype (SASP)

matrix metallopeptidases (MMP)

interleukins (IL)

synovial fluid (SF)

hyaluronic acid (HA)

nonsteroidal anti-inflammatory drugs (NSAID)

intra-articular (IA)

extracellular matrix (ECM)

Senescent Cells (SCs)

platelet-derived growth factor AA (PDGF-AA)

DNA damage response (DDR)

senescence-associated beta-galactosidase (SA-β-gal)

Anterior cruciate ligaments transection (ACLT)

tri-modal reporter (3MR)

Renilla luciferasee (rLUC)

monomeric red fluorescent protein (mRFP)

herpes simplex virus thymidine kinase (HSV-TK)

ganciclovir (GCV)

murine double minute-2 (MDM2)

National Disease Research Interchange (NDRI)

Institutional Research Board (IRB)

phosphate-buffered saline (PBS)

penicillin and streptomycin (Pen/Strep)

Dulbecco's modified Eagle's medium (DMEM)

fetal bovine serum (FBS)

Non-essential amino acids (NEAA)

Human mesenchymal stem cells (hMSCs)

fibroblast growth factor (FGF)

Mouse embryonic fibroblasts (MEF)

transforming growth factor-beta 1 (TFG-β1)

Fluorescent-Activated Cell Sorting (FACS)

Region of Interest (ROI)

Immunohistochemistry (IHC)

Osteoarthritis Research Society International (OARSI)

Real-Time Polymer Chain Reaction (RT-PCR)

Complementary DNA (cDNA)

Half-Maximal Inhibitory concentration (IC50)

Poly(lactic-co-glycolic acid) PLGA

Polyvinyl Alcohol (PVA)

scanning electronic microscope (SEM)

GROα (growth-regulated oncogene α)

ICAM-1 (intercellular adhesion molecule 1)

CCL5 (chemokine (C–C motif) ligand 5)

MIF (macrophage migration inhibitory factor)

NC (non senescent cells)

pharmokinetics (PK)

extracellular matrix (ECM)

glycosaminoglycans (GAG)

urinary bladder matix (UBM)

Polyethylene glycol (PEG)

phosphocholine (PC)

Hyaluronic Acid Binding Peptide (HAPpep)

Chapter 1: Introduction to Thesis

1.1 Osteoarthritis

Osteoarthritis (OA) is a chronic musculoskeletal disease of the joints that affects 33.6% of those 65 years of age and older in the United States [1]. OA of the knee joint in particular is the most prevalent, leading to disability in 1 out of 5 of institutionalized adults [1]. In the healthy state **(Fig.1.1),** the tibial and femoral surfaces of the knee joint are covered by articular cartilage tissue that is composed of collagen II, proteoglycans, chondrocytes and has a highly organized matrix structure that imparts viscoelastic characteristics to facilitate in biomechanical load-bearing [2]. Chondrocytes are the primary cell type in articular cartilage and they are responsible for the formation and maintenance of articular cartilage [3]. In OA **(Fig 1.1),** the articular cartilage of the joint degrades and is accompanied by thickening of the subchondral bone, synovial inflammation, and osteophyte formation due to imbalance of biological molecules that disrupt homeostasis [4]. This leads to clinical symptoms of pain, joint stiffness, loss of mobility, and functional impairment [2].

Risk factors for OA include traumatic injuries, most common in military populations with 60% of wartime injuries leading to arthritis [5,6]. High level of injury-related impact energy on the articular surface can causes post-traumatic OA (PTOA) by damage to chondrocytes and the surrounding matrix structure resulting in loss of proteoglycan content and cartilage fibrillation eventually leading to functional impairment [3,7]. Military populations have a higher incidence of OA compared to general populations majorly due to injury from land mines, blast waves, explosive ordnance, vehicle crashes, and other forms of combat [8]. Another source of OA in military personnel is service-related overuse caused by physically

demanding exercise regimes and performance in extreme environments leading to load bearing beyond the physiological range [9]. In addition, sports that involve a higher intensity of joint impact and torsional loading, such as soccer and lacrosse, also can cause injuries that lead to PTOA [3].

Another risk factor for OA is natural aging. Age-related OA is caused by molecular, mechanical, and structural changes in the articular cartilage matrix. Human chondrocytes, the primary cell type in cartilage, have decreased production of proteoglycan and aggrecan molecules [10]. Cellular senescence is also a hallmark of aging that is related to OA and involves loss of proliferative potential and expression of the senescent-associated secretory phenotype (SASP) that includes production of growth factors, cytokines, proteases, and other proteins. [11]. Chondrocyte senescence is proposed to be resultant of chronic stress, and cells isolated from older patients have been shown to produce more pro-inflammatory factors such as matrix metallopeptidases (MMP) like MMP13 and MMP3 and interleukins (IL) such as IL-1β [12]. This inflammatory environment of the OA knee joint also causes the synovial fluid (SF) between the joints to become less viscous due to degradation of hyaluronic acid (HA), which affects the ability to provide effective shock absorption and lubrication [13]. Cellular senescence and decreased joint lubrication are part of a viscous cycle that leads to reduced cartilage tensile strength and stiffness and causes fibrillation and thinning of the surface with age [10,12] **(Fig.1.2).**

1.2 Current Strategies for Treatment

Current treatments for OA range depending upon the severity of the disease. The mildest form of treatment includes lifestyle changes such as weight loss and exercise. Another form of treatment is systematic analgesic medication that includes acetaminophen, nonsteroidal

anti-inflammatory drugs (NSAID), and COX2 inhibitors [2]. These only temporarily relieve pain, and often lead to other complications such as gastrointestinal bleeding. In addition, the focus of these current drug-based treatments is also on pain relief as they lack structural-modifying efficacy. There is a lack of disease modifying anti-OA drugs and current development of these types of drugs is focused on targeting the articular cartilage tissue [2].

For a more progressed form of OA, treatment options include HA and corticosteroid injections into the intra-articular (IA) space. One primary drawback of HA injections are that they have a short residence time due to degradation by native enzymes ($t_{1/2}$=24 hours) [14]. Corticosteroid injections also have limitations including injection site complications, such as leakage, and the focus on relieving pain rather functional restoration [15].

More severe forms of interventions include biomaterial treatments, still majorly in the research stage, and total joint replacement [2]. An example of biomaterial treatment currently in research phase includes injection of extracellular matrix (ECM) intra-articularly. Proteins in ECM have been shown to have regenerative applications and therefore could have disease-modifying ability, but much research still must be done in this area [16].

1.3 Specific Aims of Thesis

The multifaceted nature of OA calls for research into a variety of different modalities to successfully be able to treat the disease. The presented work will explore three different therapeutic strategies addressing limitations of current treatments, with the combined goal of assessing clinical potential through disease-modification by targeting the articular cartilage tissue and systematic pain relief:

Specific Aim 1: Further investigate the relationship between the presence of senescent cells on the healthy joint environment and how this can be attributed to OA. In addition, determine if use of a senolytic drug to clear senescent cells has disease-modifying capability using a preclinical small animal model of PTOA.

Specific Aim 2: Determine if particulate ECM injected IA into a preclinical small animal model of PTOA has disease-modifying ability and can be used as a treatment for OA.

Specific Aim 3: Utilize a hyaluronic acid binding peptide system to increase the retention of HA in the IA space and determine the therapeutic efficacy in a preclinical small animal model of PTOA.

1.4 Figures

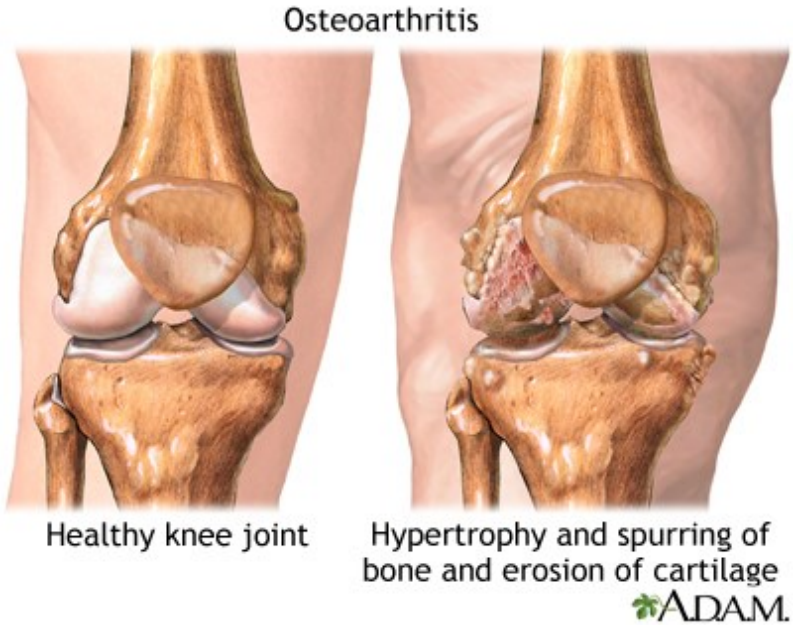

Figure 1.1 Healthy vs. OA State of the Knee Joint [17]
In the healthy joint, the articular cartilage acts as a load-bearing surface, but degrades in the OA state leading to swelling and hypertrophy of the bone.

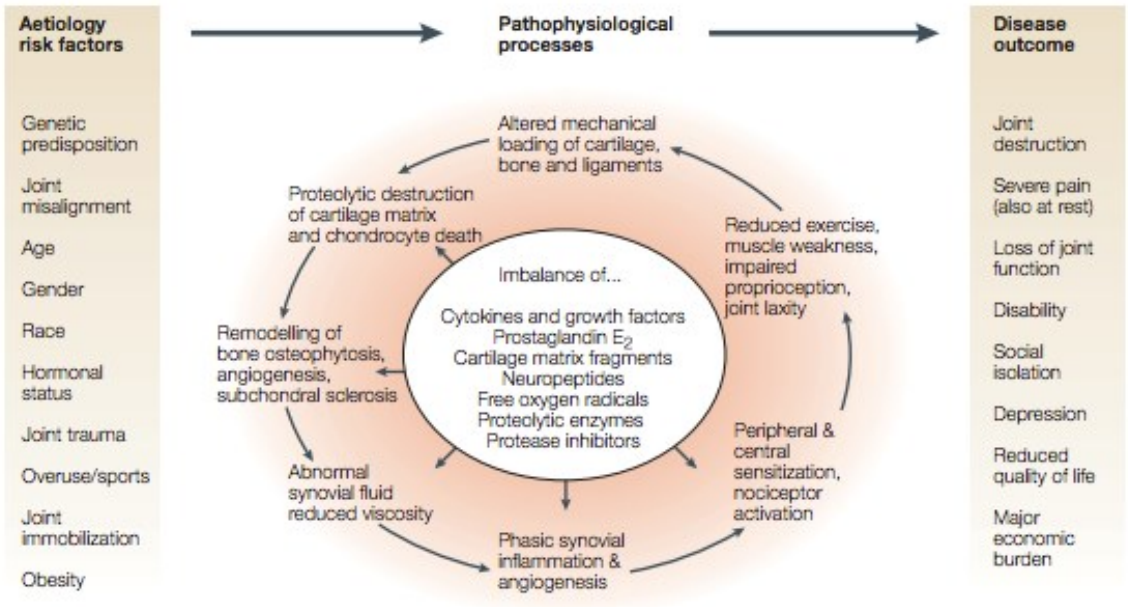

Figure 1.2 Viscous Cycle of OA [2]

There are many risk factors for OA that together create multiple pathophysiological processes such as cartilage matrix degradation and reducing viscosity of synovial fluid that eventually lead to joint destruction and clinical symptoms.

1.5 References

[1] Osteoarthritis (OA). (2015). Retrieved March 05, 2016, from http://www.cdc.gov/arthritis/basics/osteoarthritis.htm

[2] Wieland, H. A., Michaelis, M., Kirschbaum, B. J., & Rudolphi, K. A. (2005). Osteoarthritis—an untreatable disease?. Nature reviews Drug discovery, 4(4), 331-344.

[3] Buckwalter, J. A. (2003). Sports, joint injury, and posttraumatic osteoarthritis. Journal of Orthopaedic & Sports Physical Therapy, 33(10), 578-588.

[4] Blanco, F. J., & Ruiz-Romero, C. (2013). New targets for disease modifying osteoarthritis drugs: chondrogenesis and Runx1. Annals of the rheumatic diseases, 72(5), 631-634.

[5] Rivera, C. J. D., Wenke, J. C., Buckwalter, J. A., Ficke, C. J. R., & Johnson, L. A. E. (2012). Posttraumatic osteoarthritis caused by battlefield injuries: the primary source of disability in warriors. The Journal of the American Academy of Orthopaedic Surgeons, 20(0 1), S64.

[6] Greene, M. A., & Loeser, R. F. (2015). Aging-related inflammation in osteoarthritis. Osteoarthritis and Cartilage, 23(11), 1966-1971.

[7] Anderson, D. D., Chubinskaya, S., Guilak, F., Martin, J. A., Oegema, T. R., Olson, S. A., & Buckwalter, J. A. (2011). Post- traumatic osteoarthritis: Improved understanding and opportunities for early intervention. Journal of Orthopaedic Research, 29(6), 802-809.

[8] Enad, J.G. and J.D. Headrick, Orthopedic injuries in U.S. casualties treated on a hospital ship during operation Iraqi freedom. Military Medicine, 2008. 173(10): p. 1008-1013.

[9] Dominick, Kelli L., Yvonne M. Golightly, and George L. Jackson. "Arthritis prevalence and symptoms among US non-veterans, veterans, and veterans receiving Department of Veterans Affairs Healthcare." The Journal of rheumatology 33.2 (2006): 348-354.

[10] Martin, J. A., & Buckwalter, J. A. (2003). The role of chondrocyte senescence in the pathogenesis of osteoarthritis and in limiting cartilage repair. J Bone Joint Surg Am, 85(suppl 2), 106-110.

[11] Rodier, F., & Campisi, J. (2011). Four faces of cellular senescence. The Journal of cell biology, 192(4), 547-556.

[12] Loeser, R. F. (2009). Aging and osteoarthritis: the role of chondrocyte senescence and aging changes in the cartilage matrix. Osteoarthritis and Cartilage, 17(8), 971-979.

[13] Bhuanantanondh, P., Grecov, D. and Kwok, E. (2010). Rheological Study of Viscosupplements and Synovial Fluid in Patients with Osteoarthritis. *Journal of Medical and Biological Engineering*, 32(1): 12-16.

[14] Wathier, M., Lakin, B.A., Bansal, P.N., Stoddart, S.S., Synder, B.D., and Grinstaff, M.W. (2013). A large molecular weight polyanion, synthesized via ring-opening metathesis polymerization, as a lubricant for human articular cartilage. *Journal of the American Chemical Society*, 135: 4930-33.

[15] Courtney, P. and Doherty, M. (2009). Intra-articular corticosteriod injection for osteoarthritis. *International Journal of Clinical Rheumatology*, 4(6): 621.

[16] Willett, N. J., Thote, T., Lin, A. S., Moran, S., Raji, Y., Sridaran, S., ... & Guldberg, R. E. (2014). Intra-articular injection of micronized dehydrated human amnion/chorion membrane attenuates osteoarthritis development. Arthritis Res Ther, 16(1), R47.

[17] Orthopedics Center - Penn State Hershey Medical Center
http://pennstatehershey.adam.com/content.aspx?productId=115

Chapter 2: Senescent Cell Promotion of Cartilage Degradation and Clearance of Senescent Cells Prevents Development of Post-Traumatic Osteoarthritis

2.1 Introduction

2.1.1 Senescent Cells

Biological aging, termed senescence, was first observed on cells by Hayflick in the 1960s when he showed that cells have a limited number of divisions, and the number of divisions decrease with age of the donor [1]. Cellular senescence plays an important role in tumor suppression, wound healing, tissue repair, embryonic development, and aging [2]. In wound healing specifically, senescent cells (SCs) secrete platelet-derived growth factor AA (PDGF-AA) that promotes repair and reduces excessive fibrosis [3].

SCs involve an irreversible growth arrest that occurs due to external and internal stimuli and stresses, but differ from other types of non-dividing cell types [4]. Stress-inducing stimuli include telomeric DNA loss at the S stage, genomic damage at non-telomeric sites, mitogenic signaling, and hyperphysical cultural stresses, all of which lead to a DNA damage response (DDR) [4]. Although there are no specific markers for SC, the stresses cause activation of signaling networks, which ultimately lead to expression of p53 tumor suppressor, $p21^{WAF1}$, and $p16^{INK4a}$ factors which retain the senescent phenotype [2,4]. Cells that are in a temporal arrested state then transition to a senescent state by an unknown mechanism [2]. A detailed pathway of how stress leads SC can be seen in **Fig. 2.1.**

Other characteristics of the senescent phenotype include larger cellular size, expression of senescence-associated beta-galactosidase (SA-β-gal), persistent nuclear foci, and a senescent secretome termed the senescent-associated secretory phenotype (SASP) [4].

The SASP involves a robust secretion of cytokines, growth factors, proteases, and other proteins that lead to alterations in biological processes that are related to paracrine signaling such as tissue repair, angiogenesis, cellular proliferation, wound healing, and inflammation [2,4]. The composition of SASP components has plasticity across different types of cells and stress inducers [4] but it is known that some proinflammatory cytokines and chemokines are conserved between different cell types suggesting possible role of SCs in inflammatory response [2]. Although SCs may recruit immune related factors, the accumulation of SCs does not always coincide with immune cell infiltration and inflammation [2]. Based on all these characteristics of the SC phenotype, current methods to detect SC include high levels of $p16^{INK4a}$, $p21^{Waf1}$, IL-6, and SA-β-gal activity [2].

2.1.2 SCs Accumulation in Age-Related Osteoarthritis

It is known that SCs accumulate in tissues in the body that are associated with aging in chronic conditions such as OA, Alzheimer's, pulmonary fibrosis, and atherosclerosis [5,6,7]. During processes such as embryogenesis and repair, SC clearance is temporally controlled and efficient however in age-related diseases it is believed that deterioration of the immune system with age allows for SC accumulation [2]. Evidence of the connection between age-related diseases and senescence has further been explored by experiments done in targeting $p16^{Ink4a}$ positive SC in BubR1 progeroid mice [2]. In these experiments it was shown that genetically inactivating $p16^{Ink4a}$ prevents SC development and consequently reduced the onset of age-related diseases in the skeletal muscle, eye and fat tissues [2].

The relationship of how SCs are related to the progression of disease-related aging remains unknown [2]. One speculation is that cellular senescence causes a decrease in the regenerative potential of tissues and that the SASP acts on the local stem and progenitor cell

environments [4]. Another theory is that the SASP effects cellular growth, migration, and differentiation thus leading to disruption in tissue structure and function [4]. Lastly, it is believed that cytokines in the SASP lead to chronic inflammation and production of oxidants [4].

In OA in particular, the accumulation of SCs in the knee joint, mostly senescent chondrocytes, and the associated SASP further promote the disease pathology [6]. In general, chondrocytes in OA have declined mitotic and synthetic activities and make smaller aggrecan molecules and less functional link proteins [8]. Chondrocyte senescence may be due to chronic stresses generated in the local environment such as mechanical loading that induces cellular oxidative damage [8] and cytokine stimulation that causes DNA damage and subsequently telomere shortening [9]. Known SASP factors of senescent chondrocytes include matrix remodeling metalloproteases MMP3/MMP13 and pro-inflammatory cytokines interleukin-8 (IL-8), IL-6, and IL-1β [9,10]. It is believed that these factors compromise cartilage integrity due to decrease in anabolic activity [10].

2.1.3 SCs Accumulation in Post-Traumatic Osteoarthritis

Chronic stresses such as mechanical loading and cytokine stimulation can cause also lead to PTOA in addition to age-related OA. Validation of SC accumulation in PTOA was conducted previously in the Elisseeff Lab through use of a p16-3MR transgenic mouse model of PTOA induced by anterior cruciate ligament transection (ACLT). The p16-3MR transgenic mice contain a bacterial artificial chromosome with the $p16^{INK4a}$ promoter that drives expression of the tri-modal reporter (3MR) (**Fig.2.2a)** to encode a fusion protein that has Renilla luciferase (rLUC) to visualize SCs through luminescence [11]. Expression also drives the production of monomeric red fluorescent protein (mRFP) for sorting of SCs from

tissue samples and a herpes simplex virus thymidine kinase (HSV-TK) for selectively killing of $p16^{INK4a}$-expressing cells through administration of ganciclovir (GCV) that TK converts into a toxic DNA chain terminator and fragments mitochondrial DNA to induce apoptosis in SCs [11].

Measurement of luminescence through use of the rLUC fusion protein showed accumulation of SCs (**Fig. 2.2b**) and an increase in gene expression of $p16^{INK4a}$ **(Fig. 2.2c)** in the knee subject to ACLT. Additionally, the maximal accumulation of SCs, determined by luminescence and $p16^{INK4a}$ was observed to be two weeks after ACLT surgery. These results confirm that ACLT induces accumulation of SCs in the joint environment, thus providing a connection between PTOA and SCs.

2.1.4 Clearance of SCs to Treat Age-Related Diseases

As people age, they become more susceptible to chronic diseases that lead to frailty and loss of independence both of which limit healthy lifespan and the ability to live independently [12]. Current treatments for chronic conditions primarily focus on treating downstream symptoms, but do not target the cause of age-related diseases [12]. The mechanisms of aging are largely unknown, and thus it remains difficult to develop interventions to delay onset of age-related diseases [7]. Studies done in BubR1 mice have shown accumulation of SC in mice, and furthermore that inducing apoptosis of the accumulated SC in the mouse model with an administration of synthetic drug results in reduced onset of age-related diseases in the skeletal muscle, eye and fat tissues [7]. This suggests that elimination of SC could be a possible therapeutic strategy for treating age-related diseases [2]. Having mechanism-based treatments can make “aging a modifiable risk factor” [12].

There are a few strategies that can be employed to selectively eliminate SC and their SASP. One strategy includes developing antibodies to target SC through epitope recognition [12]. Some limitations of this method include complete elimination of SC, which may not be necessary since SC have also been shown to have some positive effects, and difficulty in execution that has already been a problem in the cancer field [12]. Another approach that may be promising is use of a small molecule that can be developed using high-throughout screens *in vitro* [12].

The effect of senolytic drugs has yet to be explored in context of OA. Since SC accumulate focally within the joint space in this disease, it is possible to inject senolytics into the IA space to determine how the drugs effect disease progression [12]. One possible class of small molecules that can be used are cis-imidazoline analogs, also called Nutlins, that are known to disrupt binding of the murine double minute-2 (MDM2) protein with tumor suppressor p53 [13]. Modulation of the p53 transcriptional activity activates $p21^{Waf1}$ downstream and leads to selective apoptosis of SC therefore can be potentially used therapeutically for clearance of SC [13,14].

Provided herein are the methods and results of further investigation into how SC can affect cellular processes related to OA, specifically chondrogensis and cartilage matrix formulation, and an investigation into the therapeutic effects of selectively eliminating SC through Nutlin-3a.

2.2 Materials and Methods

2.2.1 Part A: SC Promotion of Cartilage Degradation

Cell Isolation

Human articular cartilage explant samples from OA or healthy patients undergoing total knee arthroplasty or post-modem were received from the National Disease Research Interchange (NDRI; Philadelphia, PA) according to an Institutional Research Board (IRB)-approved protocol. Cartilage tissue was washed with phosphate-buffered saline (PBS) and then cut into $1mm^3$ pieces and washed 3 times with PBS supplemented with 100U/mL penicillin and 100µg/mL streptomycin (Pen/Strep). Cartilage pieces were then digested in collagenase solution (with 0.17% (w/v) type II collagenase (Worthington Biochemical, USA) in high-glucose Dulbecco's modified Eagle's medium (DMEM; Invitrogen™, Life Technologies, USA) with 10% fetal bovine serum (FBS; Thermo Fisher Scientific, USA) overnight on an shaker for 16 hours at 37°C. Filtrate was then passed through a 70uM strainer, centrifuged for 10 min at 1000rpm, and rinsed 3 times with PBS. Chondrocytes were cultured in chondrocyte growth medium composed of high-glucose DMEM supplemented with 10% FBS, 1% 100mM sodium pyruvate (Gibco™, Life Technologies, USA), 1% Pen/Strep, 1% 10mM Non-essential amino acids (NEAA; Invitrogen™, Life Technologies, USA), 1% 1M HEPES (Gibco™, Life Technologies, USA), 0.2% 0.2M L-proline, (Sigma-Aldrich, USA) and 0.2% 25mg/mL ascorbic acid (Sigma-Aldrich, USA).

Human mesenchymal stem cells (hMSCs) were obtained from Dr. Arnold Caplan (Case Western Reserve University) and maintained in MSC growth medium composed of low-glucose DMEM supplemented with 2mM L-glutamine, Pen/Strep, 10% defined FBS,

and 1.0ng/mL basic fibroblast growth factor (FGF; PeproTech, USA). Cells from passages 3-5 were used for all experiments.

Mouse embryonic fibroblasts (MEF) were isolated from pregnant 3MR transgenic mice (Buck Institute for Research on Aging, Novato, CA). On the 12-13th day of pregnancy, mice were anesthetized with 3% isoflurane and sacrificed by cervical dislocation. Mice were sprayed with 70% ethanol externally and then abdominal skin was opened and body wall was washed with 70% ethanol. Uterus was removed and placed in Petri dish with PBS. Embryos were removed from the uterus, separated from the placenta, and surrounding membrane was then transferred and rinsed in a new dish. Internal organs and head were removed using forceps and discarded while embryos were placed into individual wells of a 24-well plate and washed 4 times with PBS. Embryos were then digested overnight in individual 15 mL conical tubes at 4°C with 1 mL 0.05% trypsin (Gibco^{TM}, Life Technologies) then shaken vigorously to break up tissue and incubated at 37°C for 10 minutes. After incubation, 10mL of MEF medium (high glucose DMEM, 10% FBS, 1% NEAA, 1% Pen/Strep) was added to each embryo and mixed. Supernatant was transferred to dishes and incubated at 37°C/5%CO_2 for 3 days. P1-P2 primary MEF cells were used for all experiments.

C57BL/6 cell line MEF cells (AATC, USA) were purchased and grown in MEF medium. P3-P5 cell line MEF cells were used for all experiments.

Induction of SC by Irradiation

Cells were allowed to fully attach to tissue culture plates before irradiation. Cell plates were exposed to x-rays for a specified amount of time depending upon dosage (0 Grays=0 seconds, 10 Grays=161 seconds, 15 Grays=237 seconds, 20 Grays=314 seconds, 30

Grays=466 seconds, 40 Grays=600 seconds). Irradiation was administered via a CIXD Xstrahl machine (Xstrahl, United Kingdom) with dual x-ray tubes at a voltage of 220V and current of 13A. Cell medium was changed 1 hour after irradiation to remove detached cells. Cells were cultured for 10 days in normal culture conditions (37°C/5%CO_2) after irradiation to allow for expression of SC phenotype before using for experiments [15].

hMSC Pellet and Micromass Culture

A 2D micromass culture system was applied as previously described [16]. Cells were harvested and suspended at 2x10^7cells/mL in chondrogenic medium composed of high glucose DMEM, 1% Pen/Strep, 1% 100mM sodium pyruvate, 1% ITS premix (6.25mg/mL insulin, 6.25 mg/mL transferrin, 6.25ng/mL selenous acid; BD Biosciences, USA), 0.2% 100 nM Dexamethasone, 0.2%20 mg/mL L-proline, 0.2% 25mg/mL ascorbic acid, and 10ng/mL of transforming growth factor-beta 1 (TGF-β1; Fitzgerald Industries International, USA). Droplets (12.5µL) were placed into the center of each well in a 24-well plate and cells were allowed to adhere for 2 hours at 37°C/5%CO_2. After, 0.5mL chondrogenic medium was added to each well and changed every 3 days. 2D micromass was kept in culture for 3 weeks at 37°C/5%CO_2. 3D Pellet culture system was also applied as previously described [16,17]. hMSCs (400,000 cells) were seeded in the 96 well MicroWell™ round bottom plate (Thermo Fisher Scientific, USA) and the pellets were formed in the bottom by centrifuging at 150g for 10 min. The pellets were maintained at 37°C/5% CO_2 in 200µl of the chondrogenic growth medium for 3 weeks. The media was changed 3 times a week until the end of the experiment.

Fluorescent-Activated Cell Sorting (FACS)

Human articular chondrocytes isolated from OA patients were expanded until P3 (~20 million cells) and sorted using FACS Aria IIu Sorter (BD Biosciences, USA) based upon size in FL1 and auto-fluorescence (488 nm) by FSC as previously described [18]. There are currently no known markers of SC for live sort; therefore the sort was based enlarged size and accumulated auto-fluorescence of the age pigment lipofuscin in SC [18]. The FSC/SSC dotplot of auto-fluorescence vs. size was then generated and used to set up gates to sort the chondrocytes into three groups to generate populations with different proportions of SCs. Live cells were sorted in buffer composed of PBS with 1% FBS and collected in chondrocyte medium with 2x Pen/Strep.

Co-Culture

A 24-well Corning® Transwell® plate with 6.5 mm inserts (Sigma-Aldrich, USA) was used for co-culture experiments. Healthy chondrocytes (20,000/well) were seeded into each well. Sorted OA chondrocytes (20,000/insert) from FACS were then seeded onto the inserts. Cell were cultured for 1 week at 37°C/5%CO_2 in chondrocyte growth medium.

Bystander Effect

Healthy human chondrocytes (20,000/well) were seeded onto a 24-well plate. Conditioned medium from co-culture experiment groups (control, low, medium, high) was then added onto the cells after attachment occurred. Medium was changed once and cells were incubated at 37°C/5%CO_2 for 1 week.

SA-β-Gal Staining

SA-β-gal staining was performed using a SA–β-gal staining kit (catalog no. #K320-250, Biovision, CA, USA) according to the manufacturer's instructions. SCs were identified as green/blue-stained cells under light microscopy and counted. Total cells were counted using the DAPI staining for nuclear regions in 10 random fields on a culture dish to determine the percentage of SA-β-gal positive cells out of total cell population.

Proteoglycan Staining for 2D Culture

In vitro 2D cultures were stained for proteoglycans by adding 0.25mL of Safranin-O (0.1%, pH 5.6; Wards Chemical, USA) into each well for 5 mins and then washed with PBS 3 times. *In vitro* 2D cultures proteoglycan content was also stained with alcian blue (3%, pH 2.5; Sigma Aldrich, USA) for 30 mins then washed with PBS 3 times. Wells were then mounted and imaged under light microscopy.

Human Antibody Array

Cytokine antibody array was performed with a human cytokine array kit (R&D Systems, Catalog # ARY005) according to the manufacture's instructions. Conditioned media for antibody array analyses were prepared by washing approximately 0.2×10^6 cells once with PBS, and incubating them in serum-free medium for 24 h. The conditioned media was collected in 1.5 ml centrifuge tube and centrifuged after which supernatant placed into a new tube. Each array membrane was incubated with 1.5ml of 3-fold diluted conditioned media overnight at 4°C, washed, and incubated with biotin-conjugated antibody cocktail, washed, then incubated with streptavidin-HRP conjugate and subsequently cytokines were

detected by Chemi reagent mix. The signals developed on the X-ray film were quantified to the average signal (pixel density) of the pair of duplicate spots representing each cytokine by Image J software (NIH, USA). The experiments were repeated in duplicate.

Bioluminescence

For *in vitro* luminescence imaging, 0.2µL per 1mL of PBS of Xenolight RediJect Coelentarazine h (150µg/mlCalipers, Waltham MA, USA) was added to well of cell culture plate. Fifteen minutes later, the luminescence was measured with a PerkinElmer IVIS SpectrumCT *in vivo* imaging System (Caliper Life Sciences, Hopkinton MA, USA; 5 minute exposure, medium binning). A region of interest (ROI) was constructed around each measurement well and a background ROI was constructed to subtract from each measurement.

IA Injection

C57BL/6 mice (Charles River, Germantown, MD) that were 6-months old anesthetized were 3% isoflurane. Intra-articular injections (10µL) of 2 million irradiated MEF cells (N=5), 2 million non-irradiated MEF cells (N=5), saline (N=5), and no injection (N=5) were performed on the right knee of the mouse with a sterile 30-gauge needle. All procedures were performed according to the Institutional Animal Care and Use Committee at Johns Hopkins University School of Medicine.

Hot Plate Analysis

Mice were placed on the hotplate at 55°C (Columbus Instruments, USA). The latency period for hind limb response (includes shaking, jumping, or licking) was recorded as response time before any surgical procedures and injections, and at periods of time after the surgical procedures and injections. At least three measurements are taken per mouse. The observer was blinded to the treatment group.

Weight Bearing Analysis

Static incapacitance measurements were performed using Incapacitance Tester (Columbus Instruments, USA). Before injection, mice were acclimated to the chamber at least 3 times before measurement. After, mice were maneuvered inside chamber to stand with each hind paw on a sensor. Weight placed on each hind limb is measured over a 3-second time frame for at least 3 separate measurements. Results are expressed as a percentage of weight placed on the operated limb versus contralateral control. The observer was blinded to the treatment group.

Histological Evaluation

The pellets and knee joints were fixed in 4% paraformaldehyde overnight. Mouse joints were decalcified using 10% EDTA (Sigma Aldrich, USA) for 2-3 weeks. Successful decalcification was determined by using Calcium Colorimetric Assay Kit (BioVision, USA) according to manufacture's instructions. Joints and pellets were then dehydrated in increasing concentrations of ethanol, infiltrated with xylene, and embedded with paraffin. Seven micrometer-thick sections were cut from the paraffin block and collected onto the glass

slides. The sections were stained for proteoglycans with aqueous Safranin-O (0.1%) for 5 minutes and methyl green (Sigma Aldrich, USA) counterstain for 30 seconds then the specimens were mounted.

For immunohistochemical (IHC) staining, endogenous peroxidase of the sections was quenched using 2.5% (v/v) hydrogen peroxide in methanol and then incubated at 37°C with 0.25% (w/v) hyaluronidase for 1 h. AEC Broad Spectrum Histostain-SP Kit (Invitrogen, USA) was used following the manufacturer's instructions. Primary antibodies for $p16^{INK4a}$, type II, and X collagen, osteocalcin (Abcam, USA) were used with a 1:500, 1:300, 1:50, 1:100, dilution factor in 4% BSA dissolved in PBS.

Histological assessment of the medial tibial plateau joint was then conducted through blinded graded observations by 2 observers, according to the Osteoarthritis Research Society International (OARSI) Scoring System.

RT-PCR Analysis

To extract RNA from knee joints, the operated and control hind limbs were dissected and immediately transferred to liquid nitrogen and then pulverized with mortar and pestle and transferred to a micro centrifuge tube. Total RNA was extracted from the knee joints using the Trizol reagent and reverse transcribed to complementary DNA (cDNA) using Super-Script II reverse transcriptase following the manufacturer's protocol (Invitrogen, Carlsbad, CA).

To extract RNA from pellet samples, the samples were placed into a microcentrifuge tube and immediately transferred to liquid nitrogen before being pulverized in the tube with a pestle. Total RNA is then extracted from pellet samples and from monolayer cell cultures

using RNeasy Mini Kit according to manufacturer's protocol (Qiagen, USA) and transcribed to cDNA using Super-Script II reverse transcriptase following the manufacturer's protocol (Invitrogen, Carlsbad, CA).

Real-time PCRs for selected genes were performed using StepOnePlus Real Time PCR System with the SYBR Green PCR Master Mix. All genes are normalized to β-actin. Mouse primers are listed in **Table 1** and human primers are listed in **Table 2**. Relative gene expression was calculated by the ΔΔCt method where the ΔCt was calculated using the β-actin reference gene. ΔΔCt was calculated relative to the unoperated control group in *in vivo* studies and relative to control samples in *in vitro* studies.

Statistics

All data was statistically analyzed using one-way ANOVA with multiple comparison test in GraphPad Prism Software with an alpha value of 0.05 and 95% confidence interval with the exception of PCR data which was analyzed using unpaired t-test with Welches correction. *$p < 0.05$, **$p<0.01$, ***$p<0.001$ considered significant.

2.2.2 Part B Clearance of SC Prevents Development of PTOA

3D Chondrocyte Pellet Culture

Human chondrocytes were isolated from OA cartilage as described in **Section 2.2.1**. 3D Pellet culture system was also applied as previously described [17]. P1 OA Chondrocytes (400,000 cells) were seeded in the 96 well MicroWell™ round bottom plate (Thermo Fisher Scientific) and the pellets were formed in the bottom by centrifuging at 150g for 10 min. The

pellets were maintained at 37°C with 5% CO_2 in 200µl of the chondrogenic growth medium. Pellets were harvested after 14 days for evaluation. The media was changed every two days.

Surgically Induced PTOA model

ACLT and sham surgery were performed on 10-week or 19-month old male transgenic p16-3MR mice (Buck Institute for Research on Aging, Novato, CA), 10-week old male C57BL/6 mice (Charles River, USA), and 10-week old male Sprague-Dawley rat (Charles River, USA) as previously described [19]. Ten-week old male mice were chosen because of skeletally maturity exhibited at that age and to avoid hormonal factors with female mice [19].

To prepare for surgery, animals are placed under general anesthesia (3% isoflurane) and the hind limbs are shaved. Knee joint is exposed following a medial capsular incision and the ACL is transected with micro-scissors under surgical microscope. Open space is irrigated with saline to remove tissue debris and the skin incision is closed with sutures. The joint cavity was opened in the sham group but the ACL was not transected. All procedures were performed according to the Institutional Animal Care and Use Committee at Johns Hopkins University School of Medicine.

IA Injection

Intra-articular injections of 10µL of Nutlin-3a (1 mM), GCV (2mM), saline (vehicle), or #911(1mM, 300µM, 100 µM) were performed on the right knee of the mouse with a sterile 30-gauge needle at the appropriate dosing regime (2 weeks post-ACLT, single or multiple

injections). All procedures were performed according to the Institutional Animal Care and Use Committee at Johns Hopkins University School of Medicine.

Bioluminescence

For *in vivo* luminescence imaging, the p16-3MR mice were injected intra-articular with 10µl (150µg/ml) of Xenolight RediJect Coelentarazine h (Calipers, Waltham MA, USA). Mice were anesthesized (3% isofluorane) 25 min later and luminescence was measured with a PerkinElmer IVIS SpectrumCT *in vivo* imaging System (Caliper Life Sciences, Hopkinton MA, USA; 5 minute exposure, medium binning). A region of interest (ROI) was constructed around each measurement area and a background ROI was constructed to subtract from each measurement.

Real time RT-PCR

RT-PCR was done as described in **Section 2.2.1**. Primers were used as shown in **Table 1 and 3**.

Hotplate analysis

Hotplate analysis was done as described in **Section 2.2.1**.

Weight bearing

Weight bearing was done as described in **Section 2.2.1**. Rats were subject to the same set-up as mice.

Von Frey

Von Frey Filaments (Bioseb, USA) were used to perform static testing of pain tolerance based on paw withdrawal reflex in rats. Rats were placed on platform containing 1.5 mm diameters holes for application of von Frey hairs. Monofilaments beginning from a stiffness of 10 up to a stiffness of 60 were applied to the plantar hind paw and the level at which the rat withdrew paw was measured. At least three measurements are taken per mouse. The observer was blinded to the treatment group.

Histology

Histology was done as described in **Section 2.2.1**.

SA-β-Gal Staining

SA-β-gal staining was done as described in **Section 2.2.1**.

IC_{50} determination

Nutlin-3a was injected IA (5.8 μg/10μl) into two ACLT mice per time point (0, 0.25, 0.5, 1, 2, 4, 8, 24 hours) with each mouse providing one sample for local concentration (knee joint extraction) and one sample for systemic concentration (blood sample) measurements. Pharmokinetic measurements and determination of half-maximal inhibitory concentration (IC_{50}) was performed by Seventh Wave Laboratories (MO, USA).

Microparticle Synthesis

Nutlin-3a and ganciclovir (GCV) loaded microparticles were prepared using solvent evaporation method [20] as previously described. In brief, 20 mg of five-arm 50:50 poly(lactic-co-glycolic acid) (PLGA; Sigma Aldrich, USA) was dissolved in 2 mL of

dichloromethane for 1 hour to form the organic phase. Nutlin-3a (2 mg), GCV (2 mg), or no drug was then added to the organic phase and allowed to dissolve and mix for 1 hour at room temperature. Organic phase was then added into 1% Poly-vinyl-alcohol (PVA; Sigma-Aldrich, USA) stirring at a rate of 1000 rpm for 10 minutes to form an emulsion. The emulsion was then added to 0.5% PVA stirring at 700 rpm overnight to remove PVA. Microparticles were then collected by centrifuging, washed 5 times with distilled water, and dried by lyophilization.

In Vitro Controlled Release

Microparticles (5 mg) were placed into 1 mL of PBS in a micro centrifuge tube and placed on a shaker at 37°C/5% CO_2. A sample (0.5 ml) was taken out, measured, and replaced every 24 hours. UV/VIS Spectrophotometer (Beckman Coulter, USA) was used to measure the drug concentrations at wavelengths of 261 nm (Nutlin-3a) or 254 nm (GCV). Standard curve based on Beer's Law was created to convert absorbance to concentrations with molar extinction coefficients determined to be 0.0126 for Nutlin-3a and 0.0612 for GCV.

Encapsulation Efficiency

PLGA microparticles (5 mg) were dissolved in 2 mL DCM for 3 hours at ambient room temperature to measure the encapsulation efficiency of the particles. Concentration of drug was measured using UV/VIS Spectrophotometer (Beckman Coulter, USA) at wavelengths of 261 nm (Nutlin-3a) or 254 nm (GCV).

Scanning Electron Microscopy

To examine the surface morphology of the particles, about 0.25 mg of PLGA particles containing GCV was mounted onto a PEG and sputter coated with gold/allodium alloy to create a layer of conducting material. Particle surface was imaged using a scanning electronic microscope (SEM) (LEO/Zeiss) at 100x and 500x magnifications.

Simulation of Controlled Release

Release rate of Nutlin-3a from *in vitro* controlled release was determined from experiments. Known elimination rate from the IC_{50} studies was then incorporated to calculate the actual local concentration of the drug at a given point in time until the local concentration remained constant. Different release rates were used to determine the minimal release rate needed to sustain IC_{50} levels in the IA space for an extended period of time.

Statistics

All data was statistically analyzed in GraphPad Prism Software using unpaired t-test with welches correction where $*p < 0.05$, $**p<0.01$, $***p<0.001$ was considered significant.

2.3 Results and Discussion

2.3.1 Part A SC Promotion of Cartilage Degradation

SC Reduces Cartilage Matrix Production and Chondrogenic Differentiation Potential of hMSCs in 2D and 3D *In Vitro* Systems

MSCs are one of the potential cell types that may influence the regeneration process in damaged cartilage either directly through new cartilage tissue formation by a process

called chondrogenesis, or secretion of pro-regenerative cytokines [21, 22]. In stress related injuries such as OA, the resident MSCs in the joint have functional deficiencies in terms of altered chondrogenic differentiation and maintenance of articular cartilage tissue [21]. Previous studies have also shown that with age, the processes of differentiation, proliferation, and angiogenic potential of MSCs are reduced [1] therefore there may be an association between cellular senescence and the functional deficiencies seen in chondrogenic potential of stem cell populations in the OA knee joint [1].

To observe the impact of SCs on the chondrogenic linage potential, hMSCs were irradiated to induce senescence through DDR and kept in normal growth culture conditions for 10 days to allow full expression of SC phenotype [15] before placing into 2D/3D chondrogenic differentiation culture for 3 weeks (**Fig. 2.3a)**. Confirmation of SC phenotype development after irradiation and subsequent culture for 10 days is shown through increased presence of β-galactosides stained in the irradiated hMSCs compared to non-irradiated hMSCs **(Fig. 2.3b).** Irradiated hMSCs and control populations were then put into 3D pellet culture in chondrogenic differentiation media for 3 weeks. Confirmation of presence of SCs in the irradiated 3D pellet samples was seen by increased $p16^{INK4a}$ antibody stain and up regulation of $p16^{INK4a}$ and $p21^{Waf1}$ gene expression compared to 3D control pellet samples **(Fig. 2.3c, d).**

Overall, senescent hMSC pellets were markedly reduced in size compared to their normal, non-irradiated counterparts indicating decreased proliferative capacity, a characteristic seen in stem cell populations in OA **(Fig. 2.3c).** Safranin-O staining showed predominantly less proteoglycan content in the senescent samples of 2D micromass and 3D pellet culture systems **(Fig. 2.3c).** Control 3D pellet controls also had collagen II staining

throughout the section whereas the senescent samples did not **(Fig. 2.3c).** IHC results confirmed significant down regulation of collagen II, aggrecan, and SOX-9 gene expression **(Fig. 2.3d)** indicating the role of SCs in hindering production of cartilage extracellular matrix by altering chondrogenic differentiation potential of MSC populations.

On the contrary, Type X collagen, a marker of hypertrophic cartilage, and osteocalcin, a noncollagenous marker of bone, stained intensely throughout the senescent pellet **(Fig. 2.3c).** Particularly since a hallmark of late stage OA is thickening of the subchondral bone and development of boney osteophytes, the role of senescent MSCs in producing bone related factors, even in chondrogenic culture conditions suggests these cells may play a critical role in OA and even other cases of dysfunctional endochondral ossification after injury.

During early-stage of OA, repair is initiated by stimulation of cytokines, which eventually becomes chronic and leads to synthesis of collagenases and aggrecanases that degrade the matrix and lead to expression of markers of endochondral ossification [1]. SCs have a SASP that includes secretion of cytokines, and thus might contribute to the changes seen in the in the cartilage matrix formation in the chronic state of OA. Gene expression of IL-1β and MMP3 were elevated in the senescent 3D pellet compared to the control 3D pellet, but was not statically significant **(Fig. 2.3d).** Previous studies however have shown that irradiation induced SC hMSCs have higher levels of a large array of inflammatory mediators compared to normal hMSC cells [15]. Secretion of inflammatory mediators may be how SCs alter chondrogenic differentiation potential of surrounding stem cell populations while reducing cartilage matrix production leading to expression of bone formation factors.

Healthy Human Chondrocytes Co-Cultured with Senescent Chondrocytes Results in Impaired Cartilage Matrix Production and Increased Senescence in Healthy Chondrocytes

The presence of SCs in the joint may lead to OA and degradation of the cartilage tissue. To understand how senescent chondrocytes may impact healthy chondrocytes in the joint, a co-culture model was employed *in vitro* where varying concentrations of human primary senescent chondrocytes isolated from an OA cartilage sample were cultured with human primary healthy chondrocytes isolated from a healthy cartilage sample for 1 week **(Fig. 2.4b)**.

Primary human chondrocytes were isolated from cartilage tissues from healthy and osteoarthritic patients for use within *in vitro* experiments. In order to assess the amount of SC intrinsically present in the samples, SA-β-Gal staining was performed on cartilage explants isolated from a normal cartilage sample and OA cartilage sample. SA-β-Gal was more prominently stained in the OA cartilage explant compared to the healthy cartilage explant indicating a higher percentage of SCs **(Fig. 2.5)**. Primary cells were also isolated from a healthy cartilage sample and OA cartilage sample to determine if the cell isolation process caused spontaneous senescence in the chondrocytes. SA-β-Gal staining showed that there were 7% of SA-β-Gal positive cells in the healthy population and 44% of SA-β-gal positive cells in the OA population **(Fig. 2.5)**, therefore showing a minimal level of spontaneous senescence due to cell culture.

Chondrocytes isolated from an OA cartilage sample are a mixed population of healthy and SCs, as shown in **Fig. 2.5**, and there are currently no specific surface markers for sorting live SCs [16]. In order generate a SC enriched populations, the mixed chondrocyte population

isolated from the OA cartilage was sorted into three populations based on size and auto-florescence [18] which correlated with the level of senescence determined by SA-β-gal staining **(Fig. 2.4a)**. The resulting sorting populations contained different percentages of SCs (Low: 26.3%, Medium: 46.9%, High: 65.6%) **(Fig. 2.4a)** and were cultured with healthy chondrocytes to observe a possible SC dose response.

Healthy primary chondrocytes exposed to high percentage (65.6%) of SCs showed significant increases in $p16^{INK4a}$ mRNA levels and decreases in chondrogenesis as defined by proteoglycan Safranin O staining and collagen II gene expression level, as compared to control **(Fig. 2.4c, d)**. Elevated expression of $p16^{INK4a}$ is related to increases in MMP3 and MMP13, both of which play an integral role in OA pathogenesis [23], showing consistency with the up regulation of MMP3 expression in high (65.6%) group **(Fig. 2.4d).** Also, affirming the spread of senescence to healthy chondrocytes from exposure to high percentage (65.6%) of SC was an almost two-fold increase in $p21^{Waf1}$ gene expression compared to control **(Fig. 2.4d).**

A SC dose response of $p16^{INK4a}$, $p21^{Waf1}$, MMP3, and collagen II expression was observed with the different percentages of SCs, mimicking the age-related accumulation of SCs in OA. This suggests that a larger amount of SCs could cause a more detrimental effect on cartilage matrix production and elicit a stronger chronic effect of spreading senescence by SASP.

Healthy Human Chondrocytes Cultured with SC Conditioned Media Results in Impaired Cartilage ECM Production and Increased Senescence through Bystander Effect of SASPs

To further assess the effect of SC SASP on healthy human chondrocytes, cell medium conditioned from the various SC population groups (control, low, medium, high) in the co-culture experiment was collected and added onto a monolayer of healthy human chondrocytes in culture for 1 week **(Fig. 2.6a).** Interestingly, healthy chondrocytes grown in high, medium, and low percentages of SCs conditioned medium for 1 week showed down-regulation of proteoglycan production confirmed by Safranin-O and Alcian blue staining while exhibiting an increase of SA-β-gal-positive cells in a SC dose dependent manner **(Fig. 2.6c)**. Quantitative measure of proteoglycan stains and SA-β-gal-positive cells show significance between the control and high SC percentage (65.6%) groups **(Fig. 2.6d).**

To determine if senescence can be transmitted to the healthy chondrocytes surrounding the senescent secretory cell in non-cell-autonomous fashion, the levels of 36 secreted proteins were measured using conditioned media from the control and high SC percentage (65.5%) groups by a human cytokine antibody array **(Fig. 2.6b)**. It is noteworthy that many of factors such as GROα (growth-regulated oncogene α), IL-1α, IL-1β, IL-6, ICAM-1 (intercellular adhesion molecule 1), CCL5 (chemokine (C–C motif) ligand 5), and MIF (macrophage migration inhibitory factor) have been previously reported to be part of SC SASP [24,25]. These findings suggested that senescent chondrocytes could induce a bystander effect, spreading senescence to their neighboring healthy chondrocytes through SASP and, ultimately, contribute to the decline in their abilities to repair damaged cartilage during OA

progression. This bystander effect therefore may also contribute to the increase frequency of SC present in the knee joint with age [26].

IA SC Injection into Healthy Articular joint in C57BL/6 Mice Leads to Age-Related Progression of OA by Symptomatic Pain and Reduced Proteoglycan Production

We have seen that SC are capable of impacting cartilage formation *in vitro*, and it is known in osteoarthritic conditions that there is an accumulation of SC *in vivo*. One question that remains however is whether introducing SC *in vivo* can impact the healthy joint environment and thus relate SCs to the development of OA in an age-related model.

The irradiation and induction of MEF cells was evaluated *in vitro* before *in vivo* injection of SCs. MEF cells were isolated from transgenic 3MR mice and irradiated at 10 and 20 grays to induce SC. Induction of senescence was confirmed by bioluminescent measurements that showed that increasing irradiation induces a larger population of SC and additionally showed that P3 MEF cells had a higher luminescent signal than P1 luminescent cells indicating replicative senescence **(Fig. 2.7a).** Further confirmation of the dosage effects of irradiation was conducted on cell line MEF cells and an increase in irradiation was accompanied by an increase in SA-β-gal-positive cells and decrease in cell viability **(Fig. 2.7b).**

To avoid replicative senescence more common in the primary 3MR MEF cells irradiated and non-irradiated cell line MEF cells were injected into 6-month old CBL57 mice to determine the effect of introducing SC into a healthy joint environment **(Fig. 2.8a).** Functional pain tests were conducted every two weeks and animals were harvested at 8 weeks for further analysis **(Fig. 2.8a).**

Hot plate pain analysis showed an increase in response time in SC treated animals compared to non-senescent cell (NC), saline (vehicle), and wild-type (WT) groups paralleling the weight bearing pain analysis that showed a lower % weight put on the injected leg over the contralateral leg in the SC treated animals compared to NC, vehicle, and WT groups **(Fig. 2.8b)**. Over time, weight bearing and hot plate testing show a gradual increase in pain in the SC group compared to other groups as well **(Fig. 2.8b)**. Safranin-O staining on the medial femoral and tibial surfaces was greatly reduced in the SC treated group indicating loss of proteoglycan content **(Fig. 2.8c).** Gene expression of injected knee joint showed up regulation of $p16^{INK4a}$, $p21^{Waf1}$, MMP13, IL-1β and down regulation of collagen II and aggrecan in SC treated group compared to other groups **(Fig. 2.8d).**

These findings suggest that presence of SC in the intra-articular space can cause neighboring cells, perhaps through SASP factors such as MMP13 and IL-1β, to become senescent further causing damage to the cartilage matrix by loss of proteoglycans and reduction of collagen II production. SC can additionally induce adjacent cells to become senescent by contact via gap junction-mediated cell-cell contact and processes involving reactive oxygen species [26]. This agrees with results seen from co-culture and bystander experiments *in vitro* and highlights the importance of SASP.

2.3.2 Part B Clearance of SC Prevents PTOA

Nutlin-3a eliminates SCs in *in vitro* 3D chondrocyte pellet

We have seen that accumulation and presence of SCs is related to progression of OA through reduction of the regenerative capacity of chondrocytes, limiting cartilage matrix production. One potential strategy to treat OA therefore is to eliminate SCs through use of

senolytics, small molecules that selectively kill SCs. As there are many senolytics, and in order to begin this investigation, it was first necessary to screen senolytics with chondrocytes *in vitro* to evaluate potential candidates for OA treatment.

Five senolytics at different concentrations were screened *in vitro* with a 3D pellet culture of OA human chondrocytes by measuring SA-β-gal positive cells after treatment **(Fig. 2.9).** 3D Culture was chosen because chondrocytes tend to dedifferentiate upon monolayer culture but retain phenotype in high-density aggregate cultures [27, 28]. It is to be noted that the structure, molecular weight, and name of many compounds are not reveled for intellectual property considerations. Additionally, DMSO represents a control for the drug vehicle and UNI-2010002 represents a control for inactive compound.

From the five compounds, Nutlin-3a was the most efficient at eliminating almost all SCs at 14 days by the lack of SA-β-gal positive cells seen in both the gross pellet image and section. The UNI-2010006 compounds seem to eliminate all SCs at the highest concentration, but actually is most likely toxic due to lack of viable cells seen on the sectioned image. Nutlin-3a is a potent molecule that activates the p53 pathway in cancer cells and leads to apoptosis, which is the mechanism through which it targets SCs. Nutlin-3a provides as a promising compound to further investigate whether elimination of SCs is an effective therapeutic strategy for OA *in vivo*.

Clearance of SCs by GCV treatment prevents the development of the PTOA

Before determining if Nutlin-3a was an effective senolytic for OA treatment *in vivo*, it was necessary to validate the effect on OA pathology of clearing $p16^{INK4a}$ positive cells to

assess if this is a viable treatment strategy. To determine if clearance of SCs is related to the progression of OA, GCV was injected IA 2 weeks after ACLT surgery **(Fig. 2.10a)**

Decreased luminescence level along with reduced gene expression levels of the senescence associated proteins $p16^{INK4a}$ and $p21^{Waf1}$ confirmed elimination of SCs after GCV treatment **(Fig. 2.10b, 2.10e).** Clearance of SCs by GCV also caused inhibited articular cartilage erosion and rescue of proteoglycans, resembling normal tissue with an increase in aggrecan and collagen II gene expression in comparison to untreated group **(Fig. 2.10c, 2.10e)**. OA pathology and SC accumulation was confirmed with expression of inflammatory cytokines, IL-1β and MMP13 in untreated group compared to GCV treated group **(Fig. 2.10e).** Functional testing of OA-induced pain, that is, weight bearing on the surgical limb and hotplate response analysis, revealed ACLT surgery caused mice to favor the contralateral leg over the injured leg and have an increase latency period for the injured hind limb to reach a pain threshold after placement onto a 55°C platform (**Fig. 2.10d)**. Furthermore, administration of GCV caused mice to have a more even weight distribution between both hind legs and also decreased the latency period for the pain threshold on hot plate **(Fig. 2.10d).** These results show that clearance of SCs by selective elimination of $p16^{INK4a}$ expressing cells restores cartilage integrity while reducing pain and is thus a viable strategy for treatment of OA.

SC clearance by treatment with Nutlin-3a prevents the development of PTOA and creates a pro-chondrogenic environment

The p16-3MR transgenic model exhibited accumulation of SCs following ACLT and the potential therapeutic effects of eliminating SCs from the joint space therefore use of the

ACLT animal model on C57BL/6 mouse was employed to determine the efficacy of IA injection of senolytic agent Nutlin-3a for treatment of OA **(Fig. 2.11a).** Increased cartilage formation and proteoglycan content by Safranin-O staining resulted in a lower OARSI score for Nutlin-3a treated group and shows evidence for the efficacy of IA injection of Nutlin-3a for treatment of OA **(Fig. 2.11b).** Behavioral testing of OA-induced pain showed Nutlin-3a treatment caused mice to favor the contralateral leg over the injured leg significantly less and also significantly decreased the latency period for the induced OA hind limb to reach a pain threshold compared to ACLT and Sham groups (**Fig. 2.11c)**. Coinciding with these results, mRNA expression levels encoding $p16^{INK4a}$, the SASP factors IL-6, and MMP13 and IL-1β were down regulated whereas collagen II was up regulated with Nutlin-3a treatment **(Fig. 2.11d).** No significant change in aggrecan mRNA expression was observed, which may be due to the fact that one injection may not be the optimal regime for treatment.

Modulating the number of Nutlin-3a injections could provide a further efficacious effect on OA progression. To explore this further, between zero-six injections of Nutlin-3a at 1mM was injected IA into C57BL/6 mice to observe the effect of multiple pulsatile exposures of compound to the articular space. Gene expression data showed that five and six injections of Nutlin-3a caused further decrease of senescence-related markers $p16^{INK4a}$ and inflammatory cytokines MMP13 and IL-1β while causing increase of collagen II and aggrecan gene expression compared to one injection **(Fig. 2.12a)**. Unlike results from single injection, five-six injections of Nutlin-3a stimulated proteoglycan production **(Fig. 2.12a)**. Behavioral testing results show that there is a reduction in weight placed on contralateral leg and decrease in hot plate latency time in groups that received five and six Nutlin-3a

injections **(Figure 2.12b).** Multiple injection results indicate the clinical efficacy of having sustained exposure of the joint to Nutlin-3a for an optimized period of time.

Nutlin-3a has short residence time in the joint and initial development of a sustained release formation

We found that multiple injections improved the efficacy of Nutlin-3a treatment in comparison to a single injection. To explore this further, the pharmokinetics (PK) of Nutlin-3a in the articular joint was explored and it was found that the lifetime of Nutlin-3a in the IA space is short, and the concentration of the compound falls below the half-maximal inhibitory concentration (IC_{50}) of 25μM after only 1.5 hours **(Fig. 2.13a).** Additionally, 3.3% of the dose reaches systemic circulation and never reaches the IC_{50} systemically. The short time of Nutlin-3a in the joint explains why multiple doses were more efficacious than a single dose. Short half-life also indicates a potential clinical applicability of a sustained release formulation to deliver Nutlin-3a for an extended period of time.

Preliminary work in this area involved integrating Nutlin-3a into a PLGA microparticle formation created by oil in water emulsion and observing the *in vitro* release of the compound for 10 days. Since Nutlin-3a is very hydrophobic, GCV (hydrophilic) was also encapsulated in PLGA particles as a control. The surface morphology of the GCV particles was smooth and did no have large pores, as seen by the SEM images **(Fig. 2.14a)**. The diameter the PLGA microparticles was also measured from different batches and was determined to fall within the range of 1-8 micrometers (**Fig. 2.14b**). Lastly, the encapsulation efficiency of the particles was measured and found to be 89.44% for Nutlin-3a and 13.4% for

GCV **(Fig. 2.14c).** This was expected, as GCV is hydrophilic and would require water in oil in water emulsion to have better encapsulation rather than oil in water emulsion.

In vitro release data was collected for a period of 10 days for Nutlin-3a **(Fig. 2.13b)**. Since Nutlin-3a is a large molecule, very hydrophobic, and has low aqueous solubility, the release from the PLGA microparticles was primarily bulk erosion based and thus very slow. Cumulative concentration reached the IC_{50} after 10 days, but this *in vitro* set-up does not account for the elimination of Nutlin-3a in the environment occurring at the same time and therefore does not accurately depict the true concentration that would be in the joint environment. In order to incorporate the elimination of Nutlin-3a from the environment, the concentration of Nutlin-3a in the joint was simulated by taking into consideration arbitrary release rates from the microparticles every hour and subtracting the eliminated amount of drug every 1.5 hours from this total amount until a steady concentration was reached **(Fig. 2.13c).**

It was found that based on the rate of the release of Nutlin-3a from the *in vitro* study, 0.157μM/hour, the amount of compound in the knee joint would not be able to reach the IC_{50} and therefore would not have therapeutic efficacy. It was determined that minimum rate of release of Nutlin-3a from the microparticle, or another type of release formulation, would have to be 6.5μM/hour. Possible future work in this area could include a gel-based formulation such as a hyaluronic acid gel that would quickly release the drug, using crystalized drug formulations, or increasing the drug load of the microparticles. In addition, it is to be noted that the actual release *in vivo* of the formulation may be accelerated compared to the *in vitro* release rate due to the inflammatory environment of the knee that may catabolize polymers [29].

The efficaciousness of Nutlin-3a treatment on PTOA in old mice

Aging is a risk factor for development of OA, and it would be interesting to see if SC removal in PTOA injury model in old mice results in a similar disease modification as in young mice. Transgenic p16-3MR mice 19-months in age were subject to ACLT and injected IA with Nutlin-3a.

The contralateral leg was also evaluated to learn if SCs and OA were naturally occurring with age. Luminescence results show a low level of $p16^{INK4a}$ expressing cells in the contralateral leg and safranin-o staining showed minor changes in proteoglycan content throughout the tibial plateau compared to a normal young mice resulting in an OARSI score of 2 **(Fig. 2.15a,b)**. Pain results for mice that had no surgery however were similar to that of young mice **(Fig. 2.15c)**. Together, these results show that old 3MR mice may have age-related SC accumulation in the IA joint have some cartilage depredation that could attribute to mild OA.

ACLT mice showed increase in luminescence level in addition to cartilage lesions in the medial tibial plateau and significant proteoglycan loss resulting in severe OA. In comparison Nutlin-3a treated group had a significant reduction in luminescence indicating targeting of $p16^{INK4a}$ positive cells, but had only slight improvement in proteoglycan content and OARSI scoring **(Fig. 2.15a,b).** Pain results show slight decrease in favoring the contralateral leg in weight bearing measurements and slight decrease in hot plate latency period for Nutlin-3a treated group (**Fig. 2.15c**). Decreased mRNA levels of $p16^{INK4a}$ and $p21^{Waf1}$, the SASP factors IL-6 and MMP13 was observed in Nutlin-3a treated old mice compared to ACLT group (**Fig. 2.15d)**. On the contrary, Nutlin-3a treatment did not have

significant up regulation of collagen II and aggrecan (**Fig. 2.15d)** as seen in young mice, agreeing with histological results.

Overall results show that Nutlin-3a may still target and eliminate SC in the IA space, but does not result in the same pro-chondrogenic environment as seen in young mice. One possible reason for this is that the proliferative and regenerative potential of articular chondrocytes declines with age [30]. Age is also effects basal patterns of gene expression in joint tissues and the response to surgically induced OA [31].

Nutlin-3a is efficacious in ACLT model in rat and further evaluation of other senolytics

Nutlin-3a provides as a promising senolytic for treatment of OA. One consideration however, is if the potential therapeutic advantage is just limited to the mouse model. To explore this a little bit further, a drug screen of different dosing regimens of Nutlin-3a and another senolytic compound, #911, was performed in a rat model.

The OA-induced pain was measured on the basis of weight distribution between surgery operated and contralateral legs and von Frey test that measures pain response to pressure contact. It was found that groups 3, 4, 11 had the most balanced and stable posture indicating less pain **(Fig. 2.16).** Group 3, 6, 7, 11, 12 showed increase in withdrawal threshold, showing decrease in mechanical sensitivity/pain (**Fig. 2.16**). Overall mRNA gene expression data shows that group 3 and 11 are the best treatments compared to all other compounds and regimes based on down regulation of $p16^{INK4a}$, MMP13, IL-6, IL-1β and up regulation of collagen and aggrecan (**Fig. 2.17).** These results cumulatively show that Nutlin-3a is efficacious in the rat model in addition to the mouse model, and that compound #911 may have some efficacy as well. Efficacy of compound #911 however was not

predicted by *in vitro* 3D chondrogenic pellet drug screen **(Fig. 2.9)** indicating that the drug may have a mechanism of action that is dependent on more complex biological processes then can not be mimicked *in vitro*.

2.4 Conclusion

2.4.1 Part A SC Promotion of Cartilage Degradation

The functional deficiencies in stem cell populations in the osteoarthritic knee joint can be attributed partially to senescence of mesenchyme stem cell populations causing decreased proliferative and chondrogenic potential by growth arrest and secretion of pro inflammatory cytokines. This negatively affects cartilage matrix regeneration through reduced production of collagen II and aggrecan, which could contribute to hypertrophy of the subchondral bone. In addition, indirect contact of healthy cells and SCs through co-culture model and bystander effect shows that the SASP plays an important role in how SCs affect neighboring healthy cells and can cause them to become senescence along with hindering ability to produce cartilage matrix contributing to the OA pathology. The presence of a larger portion of SCs causes a more detrimental impact and further progresses the disease of the joint. Additionally, senescence may also be related to the onset of OA as introducing SCs into the joint for a sustained time resulted in cartilage degradation, pain, and further accumulation of SCs *in vivo* indicating early-state OA.

2.4.2 Part B Clearance of SC Prevents Development of PTOA

In vitro drug screen of senolytic compounds showed that Nutlin-3a was a viable compound for the clearance of SCs. Nutlin-3a is a potent molecule that activates the p53 pathway in cancer cells and leads to apoptosis. Transgenic p16-3MR mouse model of PTOA

induced by ACLT was then used to confirm the accumulation of SCs in the knee joint and that selectively killing $p16^{INK4a}$ expressing cells reduced the progression of OA. The effect of Nutlin-3a was then evaluated *in vivo* and was found to mitigate symptomatic pain while modifying disease through generation of a pro-chondrogenic environment promoting cartilage matrix production and reducing inflammatory and SASP factors. Pharmokinetics showed that Nutlin-3a remains in the joint for a short period of time, and that multiple injections improve the efficacy of the treatment proposing the need for a sustained release formulation. Nutlin-3a was also shown to an effective treatment in rat model of PTOA, where it was shown that there are other senolytic compounds such as #911 may also be effective in the context of OA. Although Nutlin-3a produced positive results in young mice, it proved not as effective of a treatment in old mice, most likely due to reduced regenerative capacity of chondrocytes with age.

2.5 Future Directions

2.5.1 Part A SC Promotion of Cartilage Degradation

Future work to elucidate how SCs affect healthy cells in vitro can include a number of different experiments. The effect of direct contact of SCs and healthy cells would be interesting to evaluate if this further reduces chondrogenic characteristics of chondrocytes than just in direct contact. Additionally, a more in depth analysis of the SASP can be evaluate in the future to determine which particular factors are related to the contribution of age-related OA and PTOA. Lastly, the injection of SCs into the joint can be conducted again with tagged cells so that it can be determined if the cells are residing in the joint or migrating out and with a longer time point and multiple cell injections. One consideration in the

experiments performed is that artificially induced senescence, in this case through irradiation, may not be the same as natural cellular senescence. Previous studies have shown that the major SASP components between irradiated human MSCs replicative induced senescence human MSCs are conserved [14] but this should also be explored within context of OA and chondrocytes

2.5.2 Part B Clearance of SC Prevents Development of PTOA

Since efficacy of multiple Nutlin-3a treatments was observed, there is a need to develop a sustained release formulation for delivery of Nutlin-3a for an optimized timeline at the IC_{50} level. Optimized regime for treatment of older populations and age-related OA and treatment using other senolytics that could also be explored more in the future. This work also alluded to the importance of immune related factors such as pro-inflammatory cytokines and MMPs in disease pathology. Future work can include determination of the types of immune cells present in the IA joint during the progression of OA and in the treatment phase.

2.6 Figures

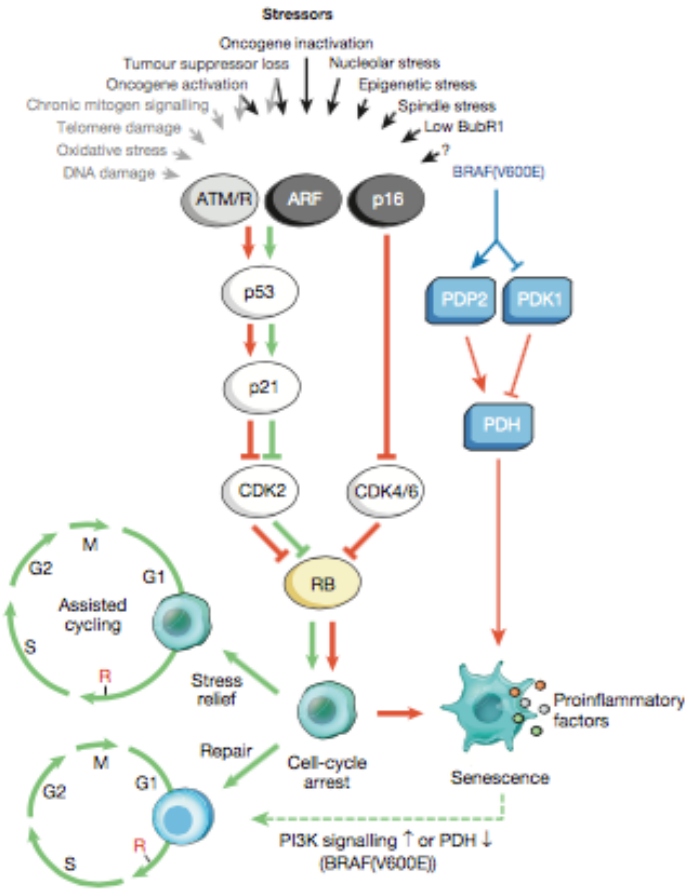

Figure 2.1 Senescence-inducing stimuli and main effector pathways [2]
Different types of internal and external stresses can lead to induction activation of $p16^{INK4a}$ and/or p53- $p21^{Waf1}$ pathways that induce senescence.

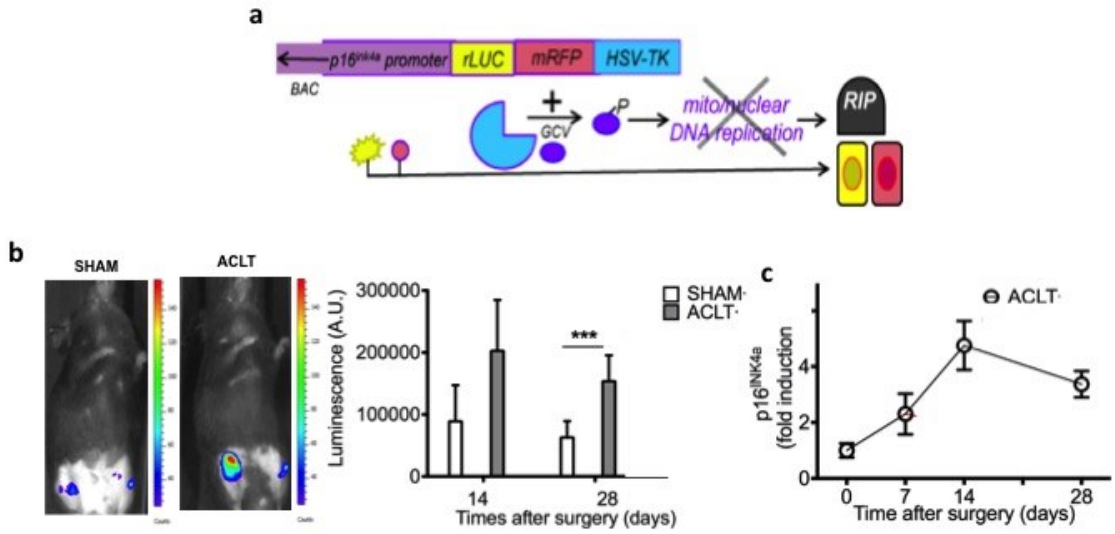

Figure 2.2 Accumulation of SC in the Knee Joint of PTOA 3MR-p16 Mouse Model
p16-3MR mice either underwent sham surgery or anterior cruciate ligament transection (ACLT). **(a)** p16-3MR transgenic mice contain a bacterial artificial chromosome with the p16INK4a promoter, luciferin and RFP imaging modalities, and herpes simplex virus thymidine kinase (HSV-TK) for selectively killing. **(b)** Representative luminescence images of sham and ACLT mice at 28 days (Left) and quantification of the luminescence at the indicated time (days) after ACLT surgery (Right). **(c)** Quantification of mRNA expression for p16INK4a in ACLT joints at the indicated time (days) after ACLT surgery.

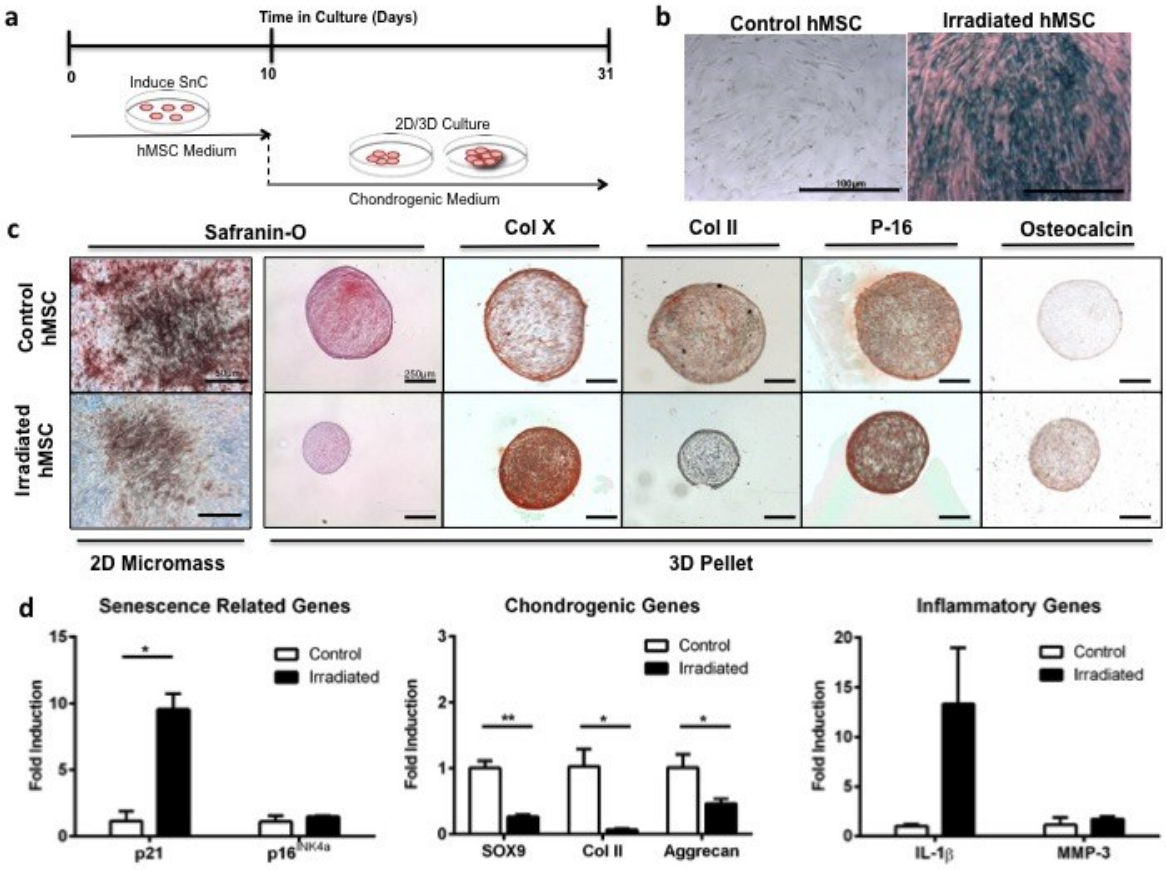

Figure 2.3 SCs impairs chondrogenic potential and reduces ECM production of human mesenchymal stem cells in 2D and 3D culture

(a) Timeline of inducing SCs and Culture in 2D and 3D systems **(b)** Confirmation of SCs induced by X-Ray Irradiation by SA-β-gal staining. **(c)** Immunohistochemical ($p16^{INK4a}$, Type II and Type X collagen (Col II and Col X), and osteocalcin (OCN)) and Safranin-O staining (2D and 3D Systems) of non-senescent or senescent hMSCs induced by irradiation. **(d)** Quantification of mRNA expression for $p16^{INK4a}$, $p21^{Waf1}$, IL-1β, MMP3, Col II, Aggrecan, SOX-9 of 3D pellet cultures of non-senescent or irradiation induced senescent hMSCs.

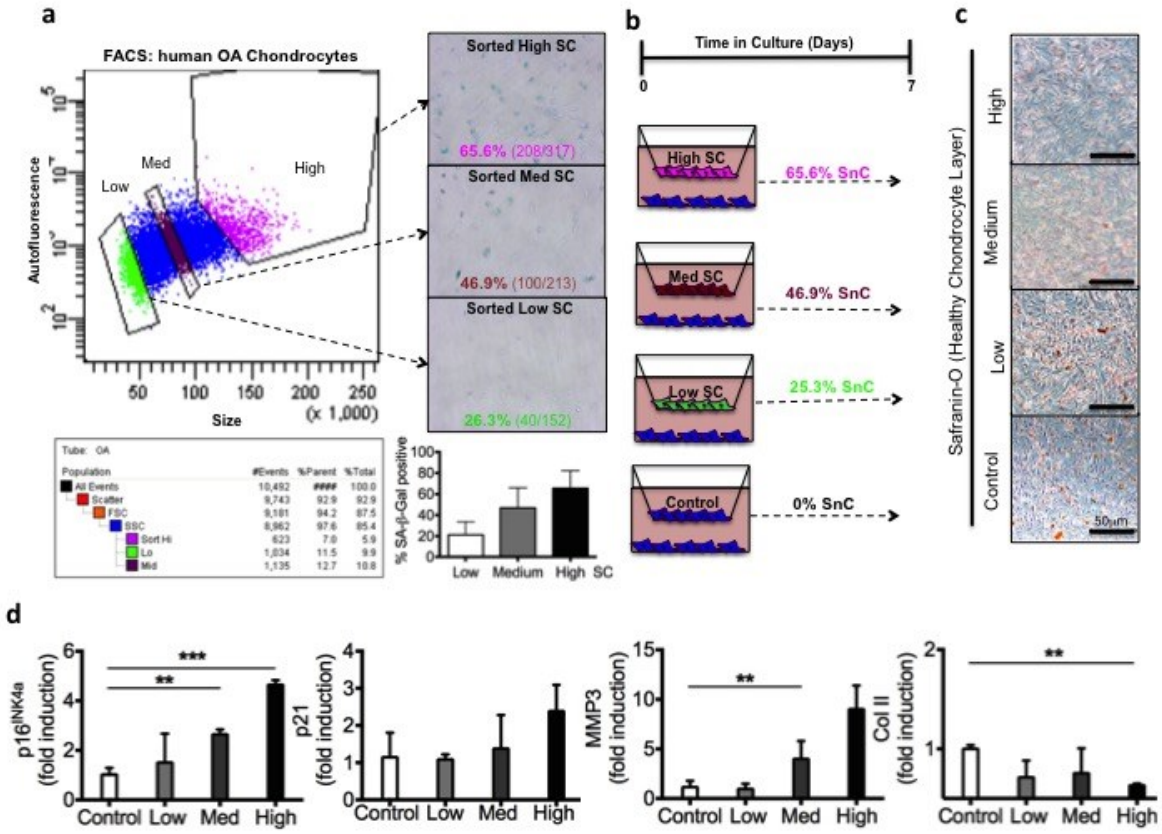

Figure 2.4 SC chondrocytes co-cultured with healthy human chondrocytes cause impaired cartilage ECM production and increased senescence of healthy chondrocyte population

(a) Gating strategy to sort senescent human OA chondrocytes from mixed non-senescent chondrocytes based on size and auto-fluorescent age pigment by flow cytometry (left) and representative SA-β-gal images of sorted cells from each gate used for co-culturing with human healthy chondrocytes (right). **(b)** Schematic of experiment for **c-d** Co-cultures where sorted High (65.6%), Med (46.9%), and Low (26.3%) SCs are placed within the insert and cultured in presence of a monolayer of healthy chondrocytes for 7 days. Control cultures contained only healthy chondrocytes. **(c)** Safranin-O staining of healthy chondrocytes that were co-cultured with different percentages of SCs. **(d)** quantification of mRNA expression for $p16^{INK4a}$, $p21^{Waf1}$, MMP3, and Col II of the healthy chondrocytes after 7 days of co-culture.

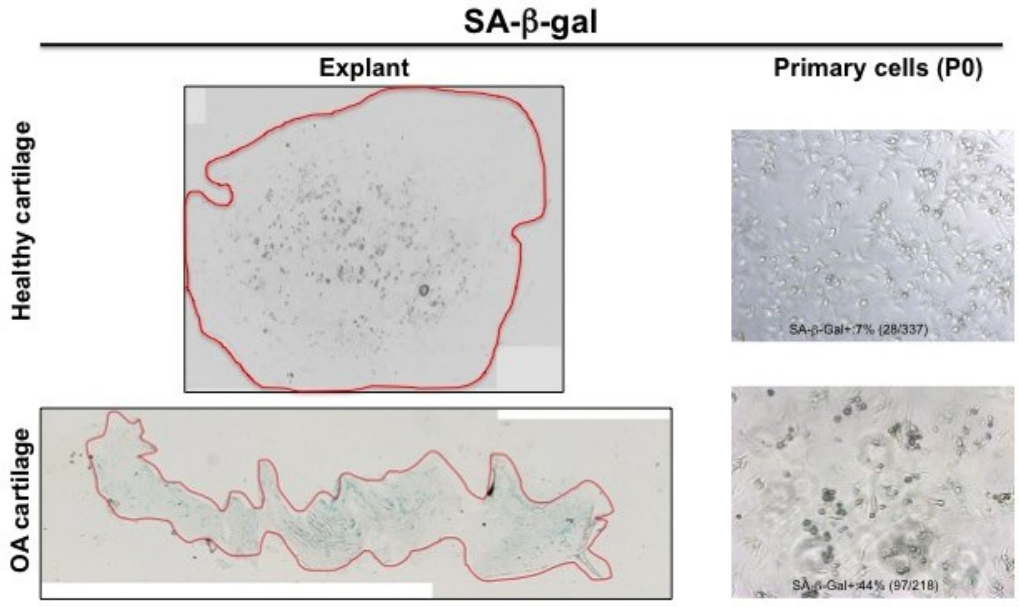

Figure 2.5 Presence of SA-β-gal-positive SCs in human healthy vs. osteoarthritic articular cartilage

SA-β-gal-positive SCs were observed throughout the depth of osteoarthritic cartilage but decreased SA-β-gal staining was present in healthy cartilage. A range of 7-15% SA-β-gal-positive SCs were observed in primary chondrocytes isolated from healthy cartilage (Passage 0) and 41–50% SA-β-gal-positive SCs were detected in primary chondrocytes isolated from osteoarthritic cartilage (Passage 0).

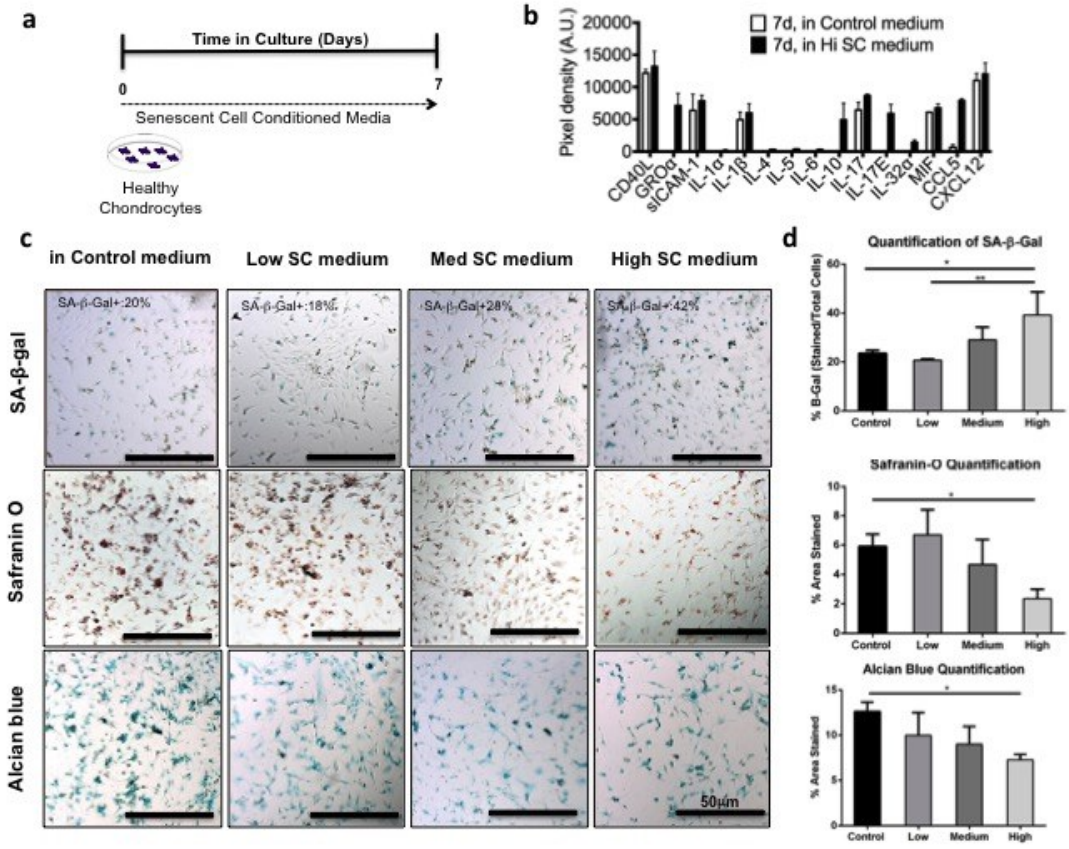

Figure 2.6 Healthy human chondrocytes cultured with SC conditioned media results in impaired cartilage ECM production and increased senescence through bystander effect of SASPs

(a) Schematic of experiment for **b-d**. Healthy human chondrocytes were cultured for 1 week with senescent cell conditioned medium from the co-culture experiment shown in **Figure 2.4**. **(b)** Conditioned media from healthy chondrocytes (Control) or High SCs was analyzed by human cytokine antibody arrays. **(c)** Induction of senescent and cartilage ECM production in healthy chondrocytes was measures by SA-β-gal, Safranin-O, and Alcian blue staining. **(d)** Quantification of SA-β-gal, Safranin-O, and Alcian blue staining.

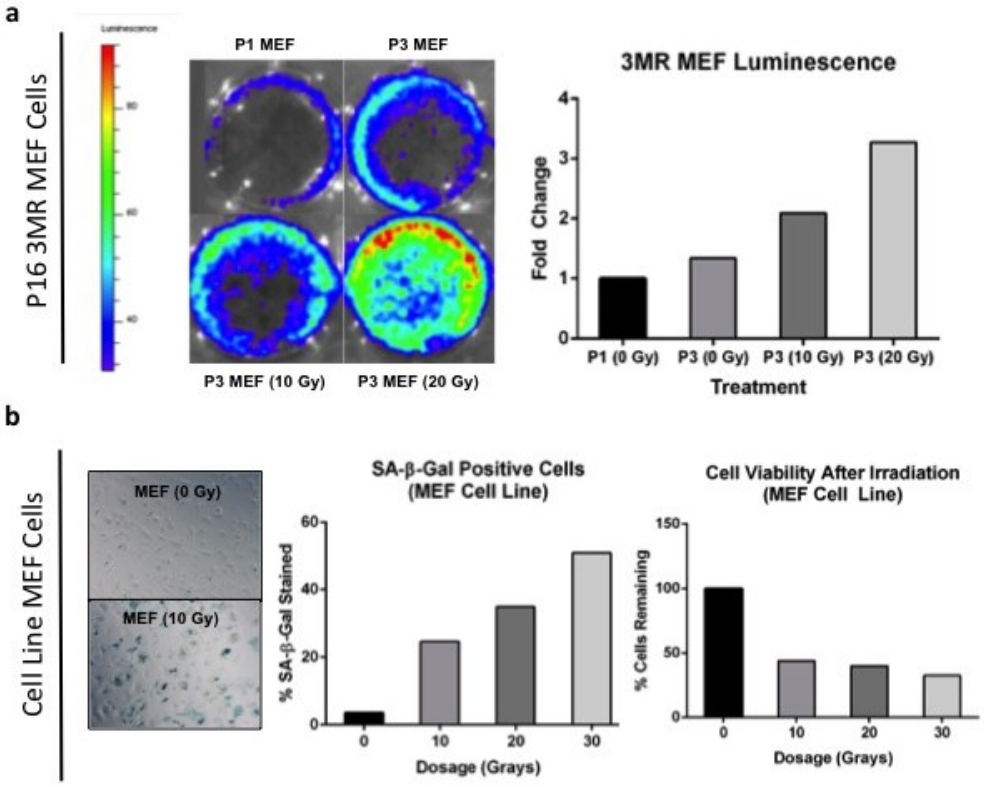

Figure 2.7 Confirmation of SC induced by irradiation in primary 3MR MEF cells and in AATC MEF cell line

(a) Confirmation of induction of SC by bioluminescent images of p16-3MR MEF Cells from non-irradiated passage 1 (P1), non-irradiated passage 3 (P3), irradiated P3 (10 Grays), and irradiated P3 (20 Grays) (left) and quantification of bioluminescence (right). **(b)** Confirmation of induction of SCs by SA-β-Gal staining (left) with quantification of SA-β-Gal positive cells at different irradiation dosages (middle) and quantification of cell viability of cells irradiated at different dosages (right).

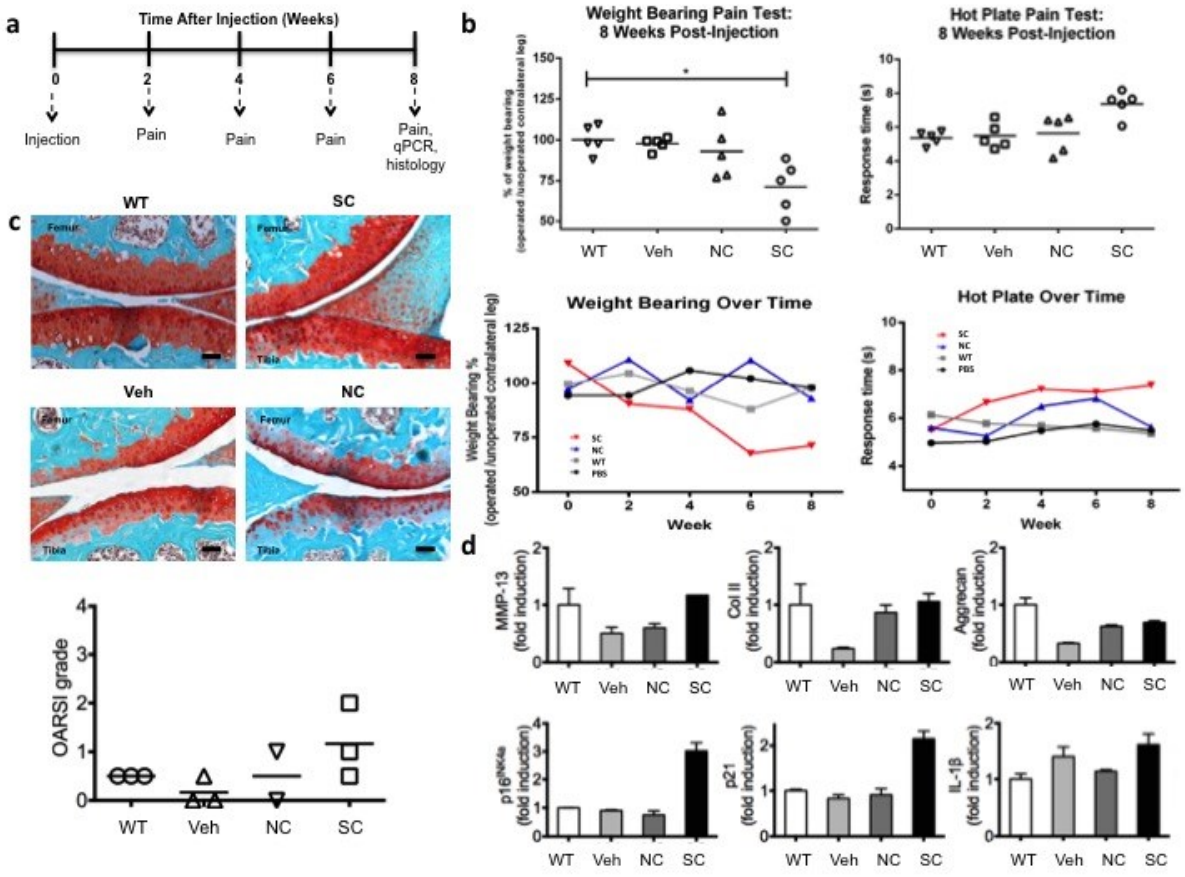

Figure 2.8 IA injection of SCs into healthy articular joint in C57BL/6 mice leads to age-related progression of OA by reduced proteoglycan production and symptomatic pain
(a) Timeline of experiment. Mice were injected with non-SC, SCs, or saline and pain was measured every 2 weeks. Mice were sacrificed for further analysis at 8 weeks. **(b)** The percentage of weight placed on the operated limb versus contralateral control and response time of mice after placement onto a 55°C hotplate on 8 weeks after SC Injection (top) and every 2 weeks for the duration of the experiment (bottom). **(c)** Representative images safranin O/methyl green from C57BL/6 mice to evaluate the pathological changes 8 weeks after SC Injection, proteoglycan (red) and bone (green) and OARSI scores. (Wild-type (WT), n=3; Vehicle-treated (Veh), n=3; senescent cell (SC) injection, n=3; non-SC (NC) injection, n=3). **(d)** Quantification of mRNA expression for $p16^{INK4a}$, $p21^{Waf1}$, MMP13, IL-1β, Col II and Aggrecan in joints from WT, Veh, SC, and NC (n=2 mice per group).

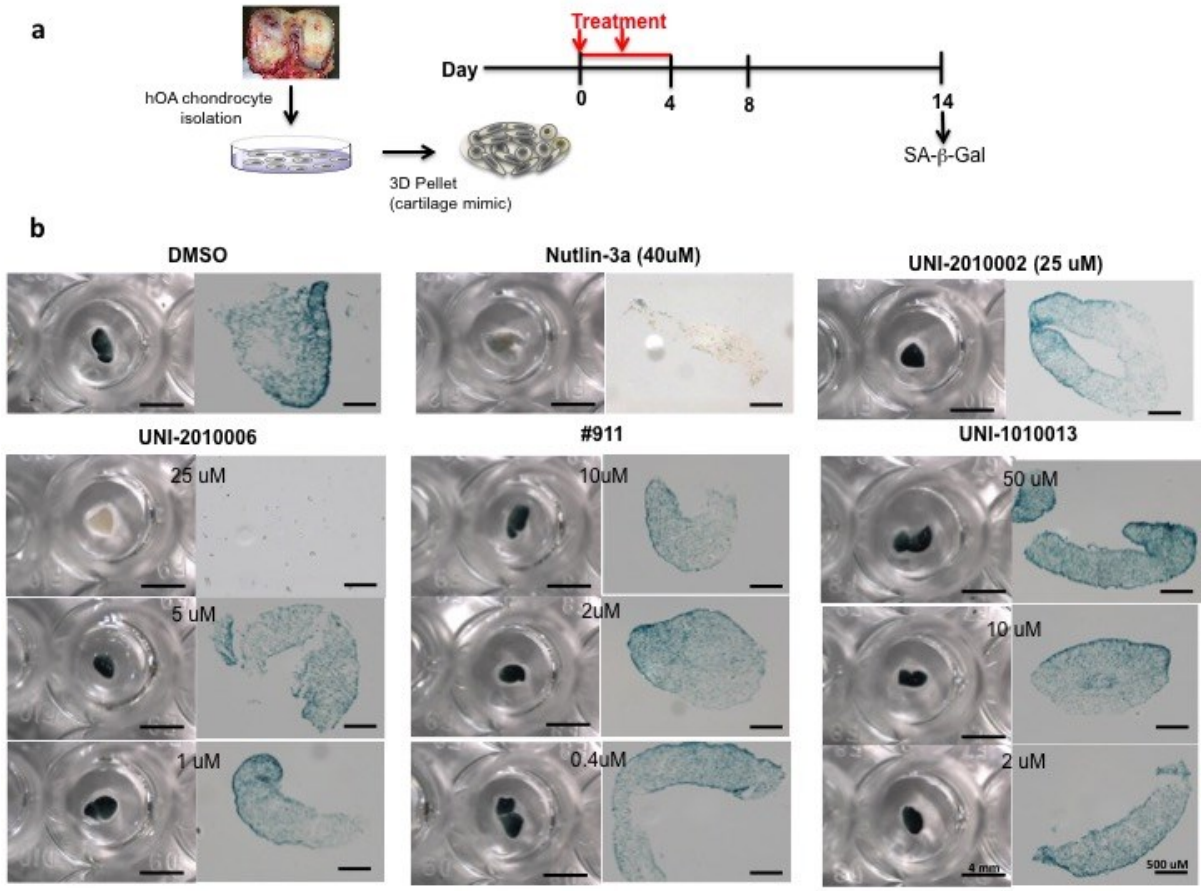

Figure 2.9 Nutlin-3a eliminates SCs in *in vitro* 3D chondrocyte pellet

3D cultured pellets of human OA chondrocytes were treated with different concentrations of senolytic compounds for 4 days and stained with SA-β-gal (Gross images (left) and sectioned images (right)) after 14 days in culture (n=2 per group).

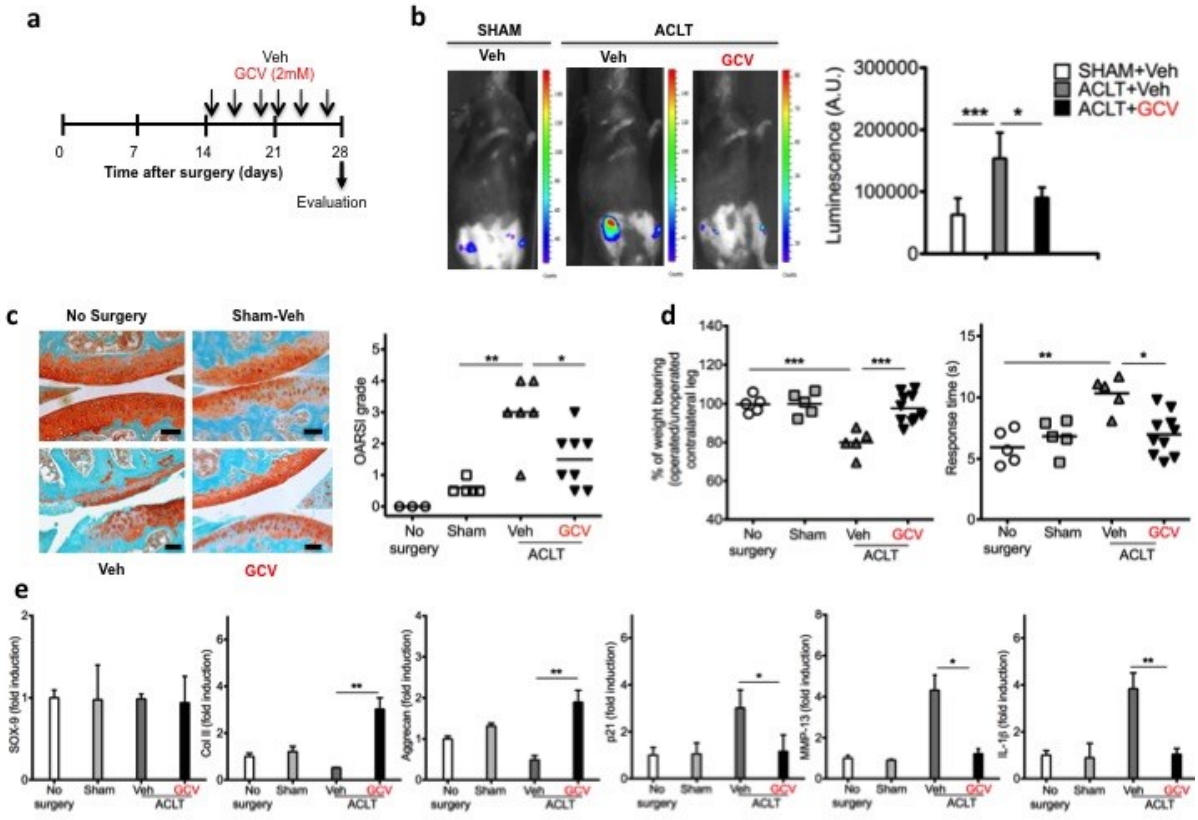

Figure 2.10 Clearance SCs by GCV treatment prevents the development of PTOA
(a) Schematic of experiment for **c-f**. p16-3MR mice undergoing the ACLT of one hind limb to induce OA was injected IA with vehicle (Veh) or gancyclovir (GCV, 2 mM) for 2 weeks. **(b)** Representative luminescence images of ACLT mice after vehicle or GCV treatment (Left) and quantification of the luminescence at the indicated time (days) after ACLT surgery (Right). **(c)** Safranin O/methyl green from p16-3MR mice to evaluate the pathological changes 4 weeks after ACLT, proteoglycan (red) and bone (green) (Left) and OARSI Scoring (Right). **(d)** The percentage of weight placed on the operated limb versus contralateral control (Left) and response time of mice after placement onto a 55°C hotplate (Right) on day 28 after ACLT surgery. **(f)** Quantification of mRNA expression for $p16^{INK4a}$, $p21^{Waf1}$, MMP13, IL-1β, Col II and Aggrecan in joints from no surgery, sham, and ACLT mice treated as indicated (n=5 mice per group).

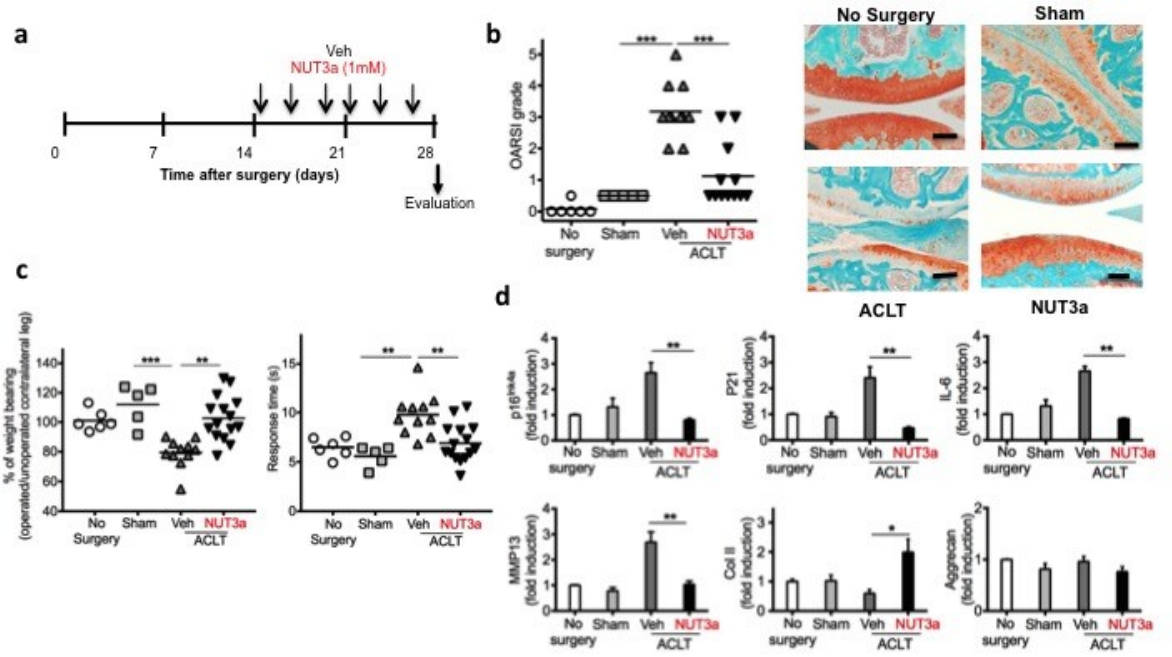

Figure 2.11 Senescence clearance by treatment with Nutlin-3a prevents the development of the post-traumatic OA and creates a pro-chondrogenic environment
(a) Schematic of experiment for **b-d**. Wildtype C57BL/6 mice underwent the anterior ACLT of one rear limb to induce OA in the joint of that limb and were injected IA with vehicle (Veh) or Nutlin 3a (NUT3a, 1mM) post-surgery for 2 weeks. **(b)** Representative images safranin O/methyl green and OARSI scores from C57BL/6 mice to evaluate the pathological changes 4 weeks after ACLT (No surgery, n=6; Sham surgery, n=5; Vehicle-treated, n=10; NUT3a-treated, n=12). **(c)** The percentage of weight placed on the operated limb versus contralateral control and response time of mice after placement onto a 55°C platform in hotplate analysis on day 28 after ACLT surgery. **(d)** Quantification of mRNA expression for $p16^{INK4a}$, MMP13, IL-1β, IL-6, Col II and aggrecan in joints as indicated (n=3 mice).

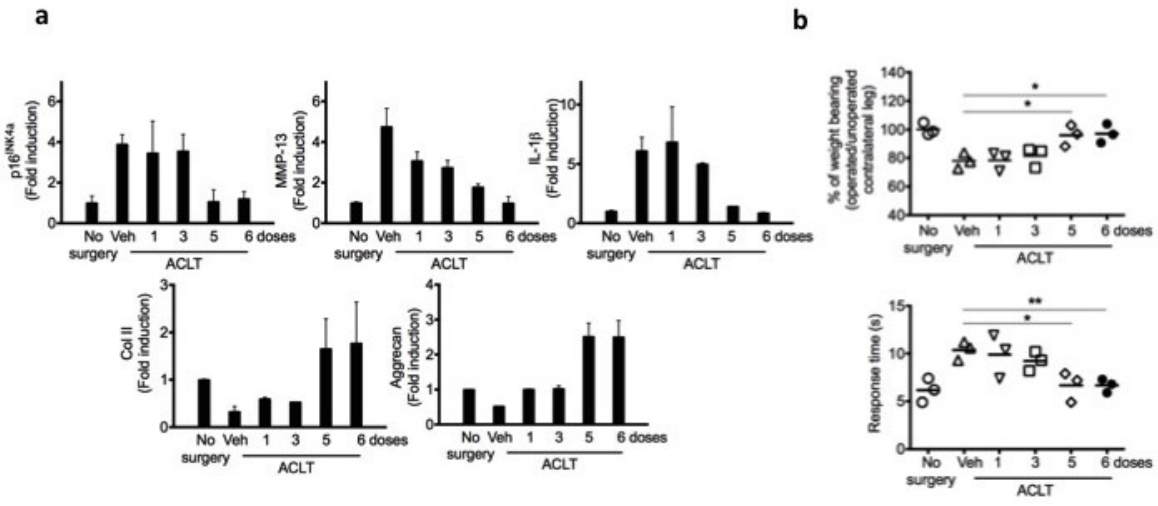

Figure 2.12 Efficaciousness of a different number of Nutlin-3a injections on OA progression

C57BL/6 mice that underwent the ACLT of one rear limb to induce OA in the joint of that limb were treated with vehicle (Veh) or a different number of Nutlin-3a intra-articular injections (1 mM, 1 to 6 injections). **(a)** Quantification of mRNA expression for $p16^{INK4a}$, MMP13, IL-1β, Col II and Aggrecan in joints 28 days after ACLT, n=2 for each group. Data are averages ± SD. **(b)** The percentage of weight placed on the operated limb versus contralateral control and response time of mice after placement onto a 55°C platform in hotplate analysis on day 56 after ACLT surgery (n=4 mice per group).

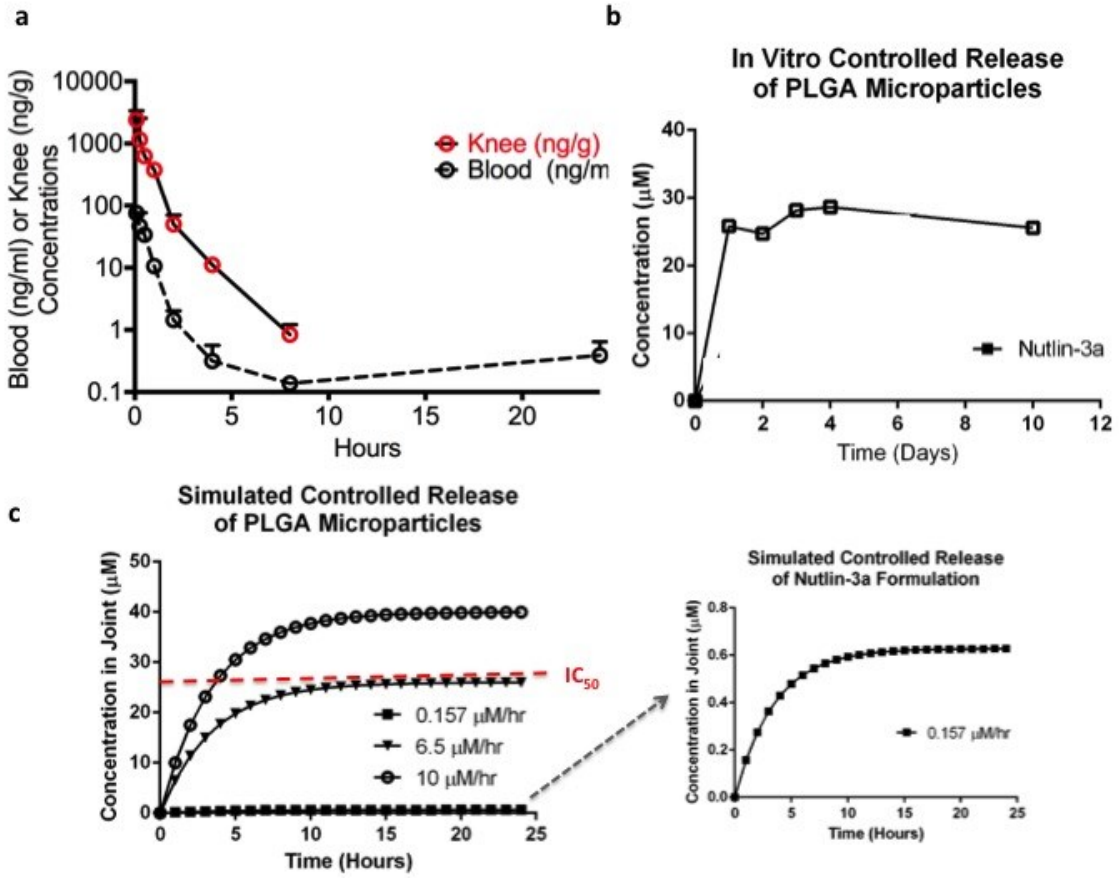

Figure 2.13 Nutlin-3a has Short Residence Time in the Joint and Initial Development of a Sustained Release Formation

(a) Local and blood Pharmacokinetics (PK) of Nutlin-3a after intra-articular injection. C57BL/6 mice were injected IA with 1mM Nutlin-3a (5.8 µg/10 µl per knee) (N=2 mice per time point). Initial dose of Nutlin-3a is below IC50 after 1.5 hour in the joint after IA injection. 1/30th of initial dose gets into systemic circulation and IC50 never reached in circulation. **(b)** *In vitro* release of Nutlin-3a from PLGA microparticles for 10 days to determine release rate (Top) and encapsulation efficiency of compounds (Bottom) **(c)** Simulation of controlled release from PLGA microparticle formulation of Nutlin-3a at different rates and predicted concentration in the joint compared to the half maximal inhibitory concentration (IC_{50}) of Nutlin-3a.

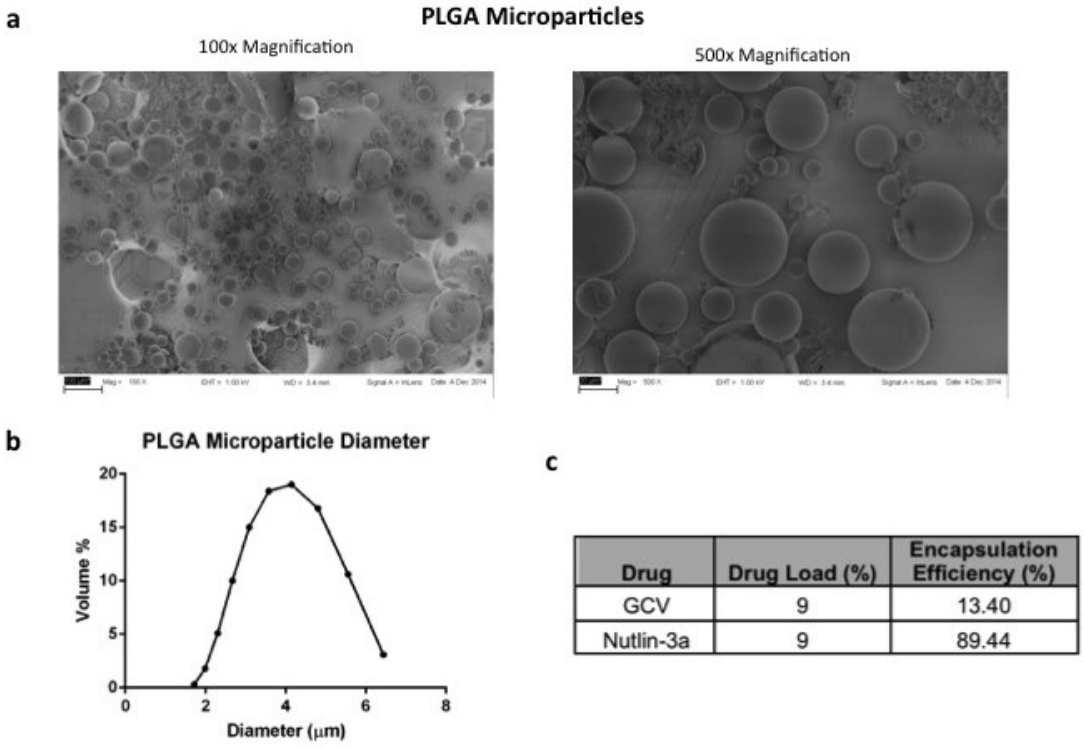

Drug	Drug Load (%)	Encapsulation Efficiency (%)
GCV	9	13.40
Nutlin-3a	9	89.44

Figure 2.14 Characterization of PLGA Drug Loaded Particles

(a) Scanning electron microscope (SEM) image of GCV loaded particles taken at 100x magnification (left) and 500x magnification (right) **(b)** Encapsulation efficiency of the drug load in GCV particle formulation and Nutlin-3a particle formation synthesized by oil in water emersion **(c)** Diameter of a volume of three different samples of PLGA particles synthesized with the same method

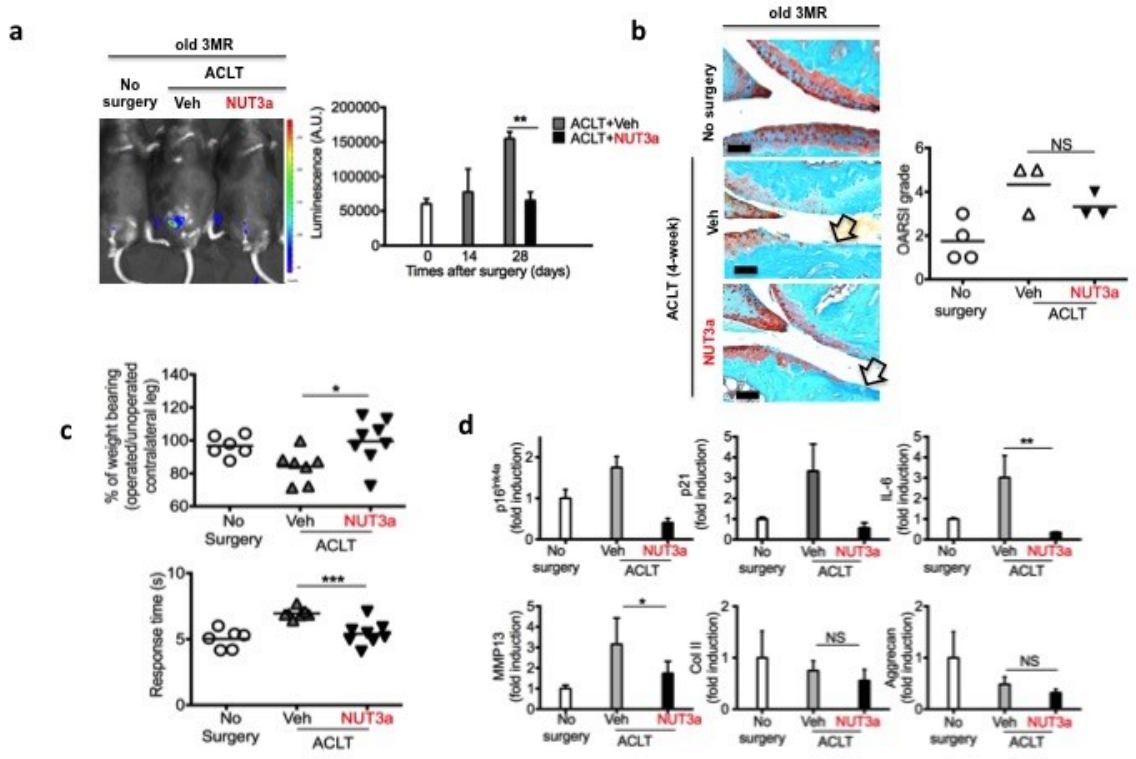

Figure 2.15 Efficaciousness of Nutlin-3a treatment on post-traumatic OA in old mice
19-month old p16-3MR that underwent the ACLT of one rear limb treated with vehicle (Veh) or Nutlin-3a (NUT3a, 1 mM) once every two days over 2 weeks starting 3 weeks post-surgery. **(a)** Representative whole body luminescent images of vehicle (Veh) or 1 mM of Nutlin-3a-treated p16–3MR mice luminescence images after 28 days following IA injection (Left) and quantification of luminescence, n=5 for each group (Right). **(b)** Representative images of Safranin O/methyl green staining of sagittal sections of the medial compartment. Black arrow indicates areas with the loss of proteoglycan at 28 days after ACLT (Left) and OARSI score (Right). **(c)** The percentage of weight placed on the operated limb versus contralateral control and response time of mice after placement onto a 55°C platform in hotplate analysis on day 28 after ACLT (n=6 for no surgery group; n=8 for vehicle-treated and Nutlin-3a treated group) **(d)** Quantification of mRNA expression for $p16^{INK4a}$, $p21^{Waf1}$, IL-6, MMP13, Col II, and Aggrecan in joints on day 28 after ACLT, n=3 for each group.

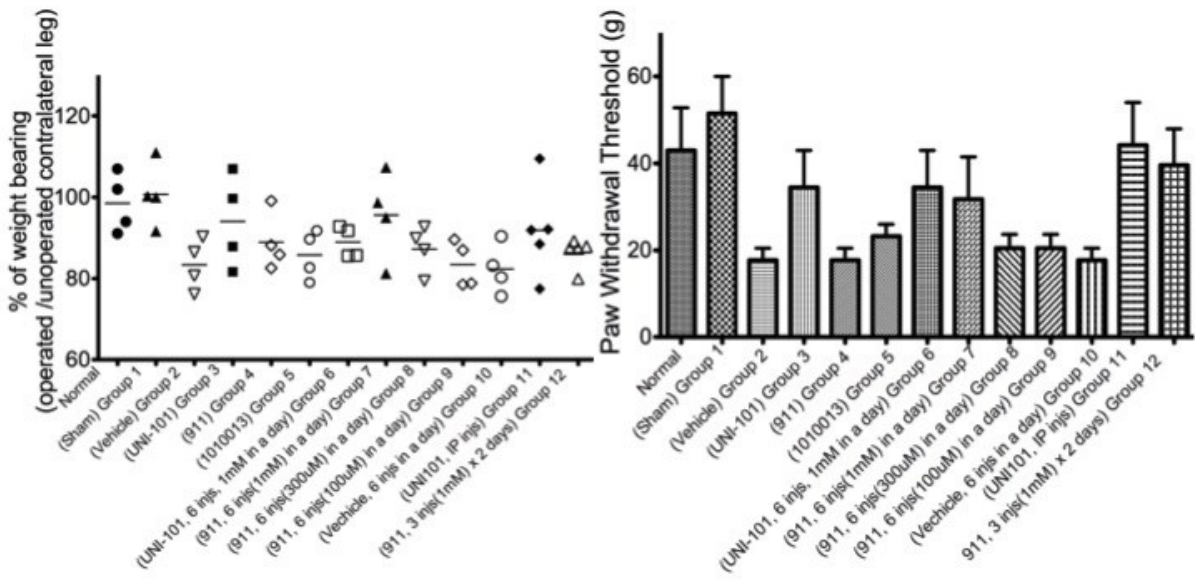

Figure 2.16 Efficacy of clearance has SCs by Nutlin-3a and #911 in treating pain in PTOA rat model

Rats that underwent the ACLT of one rear limb treated with vehicle (Veh) or Nutlin-3a or #911 at a specified regimen once every two days over 2 weeks starting 3 weeks post-surgery. OA-induced pain on the basis of weight distribution between OA surgery operated and unoperated contralateral legs was measured (Left) as well as Von Frey test for pain based on tactile sensitivity to touch/pressure by applying Von Frey monofilaments were applied to the plantar hind paw with a series of filaments that ranged in stiffness from 10 to 60. Baseline levels of withdrawal threshold averaged approximately 40 grams (Right), n=5 per group.

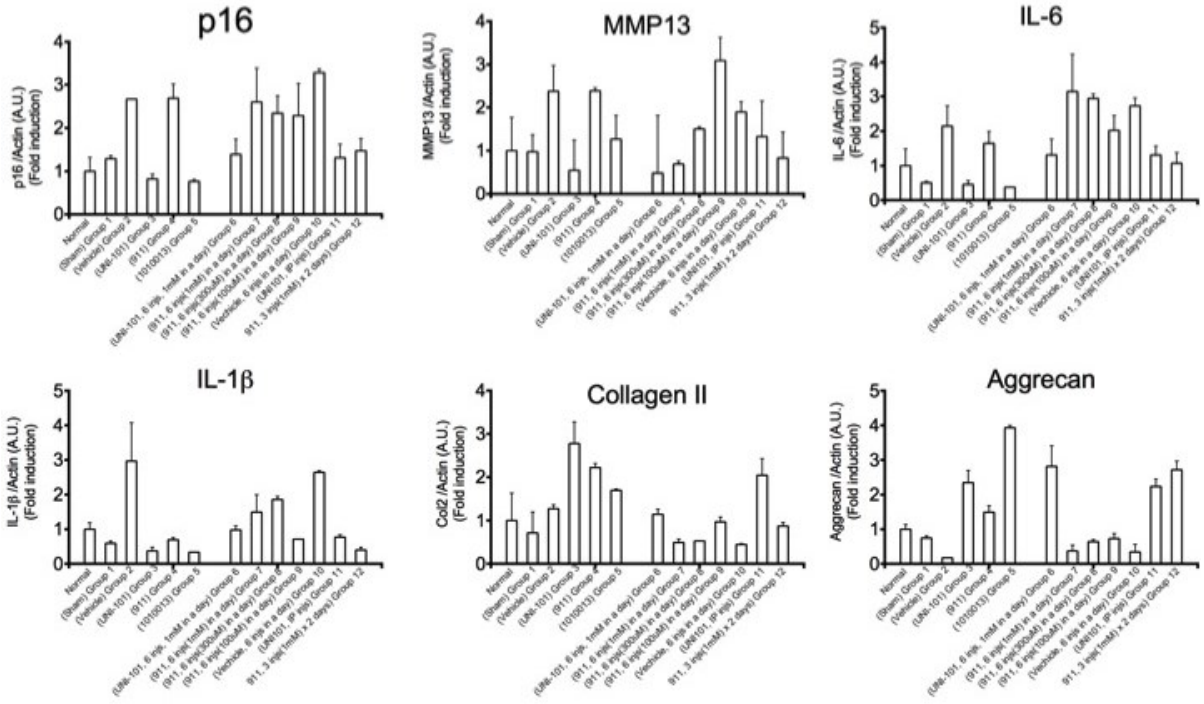

Figure 2.17 Efficacy of clearance of SCs by Nutlin-3a and #911 in treating PTOA rat model

Rats that underwent the ACLT of one rear limb treated with vehicle (Veh) or Nutlin-3a or #911 at a specified regimen once every two days over 2 weeks starting 3 weeks post-surgery. Quantification of mRNA expression for $p16^{INK4a}$, $p21^{Waf1}$, IL-6, MMP13, Col II, and Aggrecan in joints on day 28 after ACLT, n=2 for each group.

2.7 References

[1] Robert L, Fulop T (eds): Aging: Facts and Theories. Interdiscipl Top Gerontol. Basel, Karger, 2014, vol 39, pp 45–61 DOI: 10.1159/000358899

[2] van Deursen, J. M. (2014). The role of senescent cells in ageing. Nature, 509(7501), 439-446.

[3] Demaria, M. *et al.* An essential role for senescent cells in optimal wound healing through secretion of PDGF-AA. *Dev Cell* **31**, 722-733,

[4] Rodier, F., & Campisi, J. (2011). Four faces of cellular senescence. The Journal of cell biology, 192(4), 547-556.

[5] Baker, D. J., Childs, B. G., Durik, M., Wijers, M. E., Sieben, C. J., Zhong, J., ... & Khazaie, K. (2016). Naturally occurring p16Ink4a-positive cells shorten healthy lifespan. Nature, 530(7589), 184-189.

[6] Campisi, J. (2013). Aging, cellular senescence, and cancer. Annual review of physiology, 75, 685.

[7] Baker, D. J., Wijshake, T., Tchkonia, T., LeBrasseur, N. K., Childs, B. G., Van De Sluis, B., ... & van Deursen, J. M. (2011). Clearance of p16Ink4a-positive senescent cells delays ageing-associated disorders. Nature, 479(7372), 232-236.

[8] Martin, J. A., Brown, T. D., Heiner, A. D., & Buckwalter, J. A. (2004). Chondrocyte senescence, joint loading and osteoarthritis. Clinical Orthopaedics and Related Research, 427, S96-S103.

[9] Loeser, R. F. (2009). Aging and osteoarthritis: the role of chondrocyte senescence and aging changes in the cartilage matrix. Osteoarthritis and Cartilage, 17(8), 971-979.

[10] Philipot, D., Guérit, D., Platano, D., Chuchana, P., Olivotto, E., Espinoza, F., ... & Jorgensen, C. (2014). p16INK4a and its regulator miR-24 link senescence and chondrocyte terminal differentiation-associated matrix remodeling in osteoarthritis. Arthritis Res Ther, 16(1), R58.

[11] Demaria, M. et al. An essential role for senescent cells in optimal wound healing through secretion of PDGF-AA. Dev Cell 31, 722-733, doi:10.1016/j.devcel.2014.11.012 (2014).

[12] Tchkonia, T., Zhu, Y., Van Deursen, J., Campisi, J., & Kirkland, J. L. (2013). Cellular senescence and the senescent secretory phenotype: therapeutic opportunities. The Journal of clinical investigation, 123(3), 966-972.

[13] Vassilev, L. T. *et al.* In vivo activation of the p53 pathway by small-molecule antagonists of MDM2. *Science* **303**, 844-848, doi:10.1126/science.1092472 (2004).

[14] Huang, B., & Vassilev, L. T. (2009). Reduced transcriptional activity in the p53 pathway of senescent cells revealed by the MDM2 antagonist nutlin-3. Aging, 1(10), 845-854.

[15] Carlos Sepúlveda, J., Tomé, M., Eugenia Fernández, M., Delgado, M., Campisi, J., Bernad, A., & González, M. A. (2014). Cell senescence abrogates the therapeutic potential of human mesenchymal stem cells in the lethal endotoxemia model. Stem Cells, 32(7), 1865-1877.

[16] Zhang, L., Su, P., Xu, C., Yang, J., Yu, W., & Huang, D. (2010). Chondrogenic differentiation of human mesenchymal stem cells: a comparison between micromass and pellet culture systems. Biotechnology letters, 32(9), 1339-1346.

[17] Schon, B. S., Schrobback, K., van der Ven, M., Stroebel, S., Hooper, G. J., & Woodfield, T. B. F. (2012). Validation of a high-throughput microtissue fabrication process for 3D assembly of tissue engineered cartilage constructs. Cell and tissue research, 347(3), 629-642.

[18] Cell Sorting of Young and Senescent Cells
Graeme Hewitt, Thomas von Zglinicki, and Joa˜ o F. Passos

[19] Lorenz, J., & Grässel, S. (2014). Experimental osteoarthritis models in mice. Mouse Genetics: Methods and Protocols, 401-419.

[20] Bodmeier, R., & McGinity, J. W. (1988). Solvent selection in the preparation of poly (DL-lactide) microspheres prepared by the solvent evaporation method. International journal of pharmaceutics, 43(1), 179-186.

[21] Barry, F. & Murphy, M. Mesenchymal stem cells in joint disease and repair. *Nat Rev Rheumatol* **9**, 584-594, doi:10.1038/nrrheum.2013.109 (2013).

[22] van Buul, G. M. et al. Mesenchymal stem cells secrete factors that inhibit inflammatory processes in short-term osteoarthritic synovium and cartilage explant culture. Osteoarthr Cartilage 20, 1186-1196, doi:10.1016/j.joca.2012.06.003 (2012).

[23Philipot, D. *et al.* p16INK4a and its regulator miR-24 link senescence and chondrocyte terminal differentiation-associated matrix remodeling in osteoarthritis. *Arthritis Res Ther* **16**, R58, doi:10.1186/ar4494 (2014).

[24] Coppe, J. P., Desprez, P. Y., Krtolica, A. & Campisi, J. The senescence-associated secretory phenotype: the dark side of tumor suppression. *Annu Rev Pathol* **5**, 99-118, doi:10.1146/annurev-pathol-121808-102144 (2010).

[25]Cahu, J., Bustany, S. & Sola, B. Senescence-associated secretory phenotype favors the emergence of cancer stem-like cells. *Cell Death Dis* **3**, e446, doi:10.1038/cddis.2012.183 (2012).

[26] Nelson, G., Wordsworth, J., Wang, C., Jurk, D., Lawless, C., Martin- Ruiz, C., & von Zglinicki, T. (2012). A senescent cell bystander effect: senescence- induced senescence. Aging cell, 11(2), 345-349.

[27] Zhang, L., Su, P., Xu, C., Yang, J., Yu, W., & Huang, D. (2010). Chondrogenic differentiation of human mesenchymal stem cells: a comparison between micromass and pellet culture systems. Biotechnology letters, 32(9), 1339-1346.

[28] Hewitt, G., von Zglinicki, T., & Passos, J. F. (2013). Cell sorting of young and senescent cells. Biological Aging: Methods and Protocols, 31-47.

[29] Makadia, H. K., & Siegel, S. J. (2011). Poly lactic-co-glycolic acid (PLGA) as biodegradable controlled drug delivery carrier. Polymers, 3(3), 1377-1397.

[30] Loeser, R. F. Aging and osteoarthritis: the role of chondrocyte senescence and aging changes in the cartilage matrix. *Osteoarthritis Cartilage* **17**, 971-979, doi:10.1016/j.joca.2009.03.002 (2009).

[31] Loeser, R. F. *et al.* Microarray analysis reveals age-related differences in gene expression during the development of osteoarthritis in mice. *Arthritis Rheum* **64**, 705-717, doi:10.1002/art.33388 (2012).

Chapter 3. Intra-articular Injection of Matristem Reduces Development of Post-Traumatic Osteoarthritis

3.1 Introduction

3.1.1 Extracellular Matrix

The extracellular matrix (ECM) consists of tissue-specific structural and functional molecules that are secreted by resident cells of the local tissue environment [1] and is an initiator of biochemical and biomechanical cues for homeostasis, differentiation, and tissue morphogenesis [2]. Cellular products modify ECM and reciprocally the ECM signals to the cell through integrins, growth factors, and cytokines to cause metabolic and secretory changes [3]. The primary components of ECM include hydrophilic proteoglycans and structural fibrous proteins [2]. Collagen, the most abundant structural protein regulates cell adhesion and migration, directs tissue development, and imparts tensile strength [2]. Other structural proteins such as fibronectin and elastin facilitate cellular attachment and contribute to elasticity, respectively [4]. Proteoglycans are composed of glycosaminoglycans (GAG) that are attached to a polypeptide link protein and can also regulate activates of secreted proteins [4]. The highly viscoelastic properties of proteoglycans allow them to impart high compressive strength to tissues such as cartilage. Macromolecular components of the ECM are secreted primarily by fibroblasts and then degraded by MMPs [4].

3.1.2 ECM as a Biomaterial

Scaffolds composed of ECM have been shown to aid in tissue remodeling in preclinical animal and human clinical studies [1]. For example, dehydrated human amnion/chorion membrane (dHACM) has previously been studied to modulate the

development of OA and found to prevent cartilage lesions and partial erosions in addition to preventing proteoglycan loss [5]. ECM is a viable regenerative therapy for a wide-range of applications due to the presence of bioactive molecules that can drive tissue regeneration and homeostasis [3]. Natural materials such as ECM also are advantageous over synthetic materials in degradability and biocompatibility [3]. The functional outcome of ECM is dependent upon the ability to modulate the immune response, surface topology, microenvironmental cues, and growth factor retention [3].

MatriStem® is a commercially available ECM material made from urinary bladder matrix (UBM), one of the most widely studied types of ECM scaffold materials [1]. After decellularization process, the ECM contains much biochemical diversity and maintains mechanical integrity [6]. UBM specifically contains collagen VII, V, II, IV, V, VI [1] and has a luminal surface with a smooth basement membrane and an underlying surface with a mesh of connective tissue [7]. Presence of the basement membrane complex has been shown to help regulate cell growth, differentiation, and migration during tissue reconstruction [7]. Studies of macrophage polarization have also shown presence of UBM coating on polypropylene mesh induces a higher M2/M1 *in vitro* and *in vivo*, thus leading to more constructive tissue remodeling [8].

UBM has been applied clinically for treatment in open wounds allowing for skin grafting and closure [9] and in volumetric muscle loss applications resulting in promotion of muscle repair [10]. The immunomodulatory and physicochemical properties of UBM make it an attractive therapeutic for OA as well, as OA—previously regarded as a predominantly biomechanical disease [1]. The ability of UBM to have a therapeutic effect on OA was tested

by measuring inflammatory cytokine gene expression in primary chondrocytes and injecting micronized UBM into a PTOA mouse model to evaluate pathological changes.

3.2 Materials and Methods

Human Chondrocyte Isolation and Cell Culture

Human chondrocytes were isolated from OA cartilage sample as described in **Section 2.2.1**. Chondrocytes were plated in a 6-well plate (~250,000 cells/well) in chondrocyte media and incubated for 4 hours at 37°C/5%CO_2 before adding IL-1β (10ng/ml) to the media to keep the chondrocytes in inflammatory state. Cells were incubated for 16-18 hours at 37°C/5%CO_2 before addition of UBM and then incubated for 24 hours until cell isolation for PCR.

Alamar Blue Assay

Human OA chondrocytes were plated at a density of 10,000 cells/well in a 96-well plate and incubated at 37ºC until attachment occurred, after which 10ng/ml of IL-1β and varying concentrations of UBM were added to the media and allowed to incubate for 24 hours. Alamar Blue® reagent (10 µL; ThermoFisher Scientific, USA) was added directly into each well and the plate was incubated at 37ºC for 3 hours protected from light. Absorbance was measured using a microplate reader every hour for 3 hours at a wavelength of 570 nm. Data were normalized to readings at 600 nm. These measurements were used to calculate percent of Alamar Blue reduced compared to control (cells with IL-1β but no UBM).

Surgically Induced OA Mouse Model

ACLT was performed on 10-week old C57BL/6 mice as previously described in **Section 2.2.1**.

IA Injection

Two weeks post ACLT, a single 10μL IA injection of PBS (control) or UBM (50 mg/mL in PBS; pH 7.2; ACell, USA) was administered to the mice in the operated knee using a 30-guage needle (n=13 mice at 4-week time point, n=8 mice at 8-week time point).

Histological evaluation:

Histological evaluation was performed as previously described in **Section 2.2.1**.

RT-PCR analysis:

RT-PCR analysis was performed as previously described in **Section 2.2.1.** Primers are listed in **Table 1** and **Table 2**.

Weight Bearing Assessment:

Weight bearing assessment was performed as previously described in **Section 2.2.1**.

Hot Plate Assessment:

Hot Plate Assessment was performed as previously described in **Section 2.2.1**.

Statistical Analysis

Statistical analysis was conducted using one-way ANOVA test with Holm-Sidak multiple comparison in GraphPad Prism Software. $P < 0.05$ was considered significant.

3.3 Results and Discussion

UBM decreases inflammatory markers in human primary OA chondrocytes

In OA, the presence of inflammatory cytokines provokes immune cell infiltration and helps lead to disease pathology [3]. To determine the ability of UBM to have immunomodulatory capabilities, UMB was added at different concentrations onto primary human OA chondrocytes for 1 day then quantitative PCR was performed on inflammatory and catabolic markers. MMP13, a matrix-degrading enzyme involved in the progression of OA [11], as found to be significantly down regulated in the highest dose of UBM of 1μg/mL **(Fig. 3.1a).** Expression of TNF-alpha and IL-1β are also associated with OA and activate the NF-kβ signaling pathway [12]. The mRNA gene expression levels of TNF-alpha, IL-1β, and NF-κβ all showed a dose dependent decrease with increase in UBM concentration, although this was not significant **(Fig. 3.1a).** Gene expression of IL-6, another cytokine up regulated in OA [13], showed a non-significant dose dependent decrease with increase of UBM concentration **(Fig. 3.1a).** Trends of this data show that UBM could potentially help to treat OA by decreasing pro-inflammatory factors in the joint space that lead to cartilage degradation. It is possible that the decline in IL-6 and IL-1β can be attributed to the shift in macrophage towards a more regenerative environment [3] for the chondrocytes. The presence of inflammatory cytokines provokes immune cell infiltration and cause phenotypic changes in surrounding cells causing chronic inflammation that leads to disease pathology [3].

Cytotoxicity of UBM used was then tested using an alamar blue assay **(Fig. 3.1b).** The Alamar Blue assay showed that the cell viability did not change significantly compared to the control of no addition no UBM at any of the UBM concentrations.

It was observed during cell culture that the UBM particles naturally resided around the cells in the culture dish. To further investigate the interaction between the material and the cells, confocal imaging was performed 24 hours after UBM addition to the chondrocytes. Confocal imaging showed that UBM particles were not taken up by the cells **(Fig. 3.1c),** most likely due to the micron size of the particles, but were almost completely engulfed by the cell evidencing the strong interaction of these particles with cells.

UBM injection treated PTOA mice show reduced disease progression by histological analysis

In order to test the efficacy of UBM in context of OA, an ACLT mouse model was employed. ACLT was induced in mice and UBM or saline was injected in mice 2 weeks post surgery after which end point evaluation was conducted at 4 weeks and 8 weeks **(Fig 3.2a).** Proteoglycan content is essential in maintaining cartilage integrity as it contributes to its viscoelastic properties [14]. Collagen II is also an important component of the cartilage matrix as it imparts the ability to withstand tensile forces [15]. At both 4 week and 8 week time points, ACLT mice that were treated with saline exhibited proteoglycan loss **(Fig. 3.2c; arrows)** and cartilage lesions **(Fig. 3.2c; stars)** on the tibial articular cartilage. UBM treated mice had less severe cartilage lesions and more proteoglycan staining compared to the saline control at 4 weeks **(Fig. 3.2c)** and had a significantly lower OARSI score **(Fig. 3.2b).** The UBM treated group also had a significantly lower OARSI score at 8 weeks than the 8-week

saline treated control **(Fig. 3.2b),** but less proteoglycan content compared to the 4-week UBM treatment group **(Fig. 3.2c).**

Cytokines such as IL-1 and TNF-alpha are produced by synoviocytes in OA and cause MMP gene expression that lead to the breakdown of cartilage macromolecules [16]. In addition, these factors also inhibit the ability of chondrocytes to produce more cartilage matrix [16] and thus can contribute to the proteoglycan loss seen in the histology in the ACLT saline injection group. The difference between the UBM treated group at 4 weeks and 8 weeks could be attributed possible degraded of UBM and use by cells point by the MMPs present in the IA space by the 8-week time [4], and therefore the regenerative nature of the joint is unable to be maintained and returns to a more chronic state.

UBM injection treated PTOA mice show reduced inflammatory marker expression and increased cartilage matrix production

In vitro results provided a basis for observing the ability of UBM to modulate immune related factors. To explore this further, the gene expression of inflammatory and catabolic markers along with cartilage matrix factors was analyzed in the PTOA mouse model at the 4-week time point. Injection of UBM caused a significant down regulation of inflammatory markers IL-6 and IL-1β and degrading enzyme MMP13 and up regulation of anti-inflammatory markers IL-4 and IL-10 compared to saline injected mice (**Fig. 3.3**). Additionally, UBM injections also caused a significant increase in expression of cartilage ECM components collagen II and aggrecan compared to saline injected mice (**Fig. 3.3**).

In OA, the increases in inflammatory cytokines such as IL-6 and IL-1β are known to decrease aggrecan and collagen content in cartilage [17], consistent with the gene expression

data. The increase in anti-inflammatory factors in gene expression data with UBM treatment poses several beneficial effects. IL-4 has chondroprotective effects and inhibits degradation of proteoglycans by inhibiting secretion of MMPs while IL-10 stimulates collagen II and proteoglycan production, inhibits chondrocyte apoptosis and is involved in chondrocyte proliferation and differentiation [17]. Based on gene expression results, it is proposed that the UBM is facilitating modulate the immune related factors in the joint environment in a way to allows chondrocytes to rebuild tissue more efficiently. This many be why the increased proteoglycan content in the UBM treated groups at 4 and 8 weeks in the histology is observed.

UBM treatment in mice showed reduced OA-related pain

In addition to looking at the disease modifying ability of UBM injections, symptomatic pain was measured at 4 weeks and 8 weeks using functional pain testing. UBM injections significantly reduced the latency period on hot plate compared to ACLT saline injected mice at both 4 and 8 weeks (**Fig 3.4a**). The weight placed on the surgical leg over the contralateral leg at 4 weeks was significantly more evenly distributed in UBM injected mice compared to ACLT saline injected mice, which had a preference towards the contralateral un-operated leg **(Fig 3.4b).** These results correlated with the histological results **(Fig. 3.4)** and show that treatment of UBM can help relieve pain. On the other hand, the weight-bearing test did not show a significant different between the saline treated and UBM treated group at 8 weeks **(Fig 3.4b).**

Since cartilage is aneural, pain associated with OA is attributed to local changes in the subchondral bone, periosteium, synovium, joint capsule, and ligaments [18]. Pain can also

be associated with OA due to accompaniment of cytokine and substance P release, which can make secondary contributions to joint inflammation and pathology [18]. Therefore, the histological evidence and pain testing together show the reduction in OA progression with UBM injections at 4 weeks and 8 weeks.

3.4 Conclusion

UBM supports tissue formation rather than forming inferior and less functional scar tissue as would naturally occur in post-traumatic injury. Addition of UBM onto chondrocytes *in vitro* showed that UBM lowers levels of inflammatory cytokines and MMPs therefore potentially lowering the number of M1 macrophage phenotypes. *In vivo* injection of UBM in PTOA model furthermore showed the immune modulatory capacity of UBM by reduction in pro-inflammatory cytokines and increase in anti-inflammatory mediators resulting in increases in collagen and aggrecan. *In vivo* UBM injections additionally encouraged the development of proteoglycans both short-term at 4 weeks and long-term at 8 weeks, which correlated with reduced symptomatic pain. Particulate UBM has regenerative capacities when injected IA into OA knee joint and promotes generation of cartilage tissue matrix potentially through modulation of immune related cytokines and factors.

3.5 Future Directions

Future in vitro work can include doing a macrophage polarization assay to determine if UBM causes higher ratio of M2 to M1 macrophages therefore promoting tissue regeneration. Additionally, it would be interesting to see if chondrocytes cultured in UBM causes up regulation of collagen II and proteoglycans like aggrecan in a more long-term *in vitro* study. In addition, it was observed that there was a rescue of proteoglycan content and cartilage lesions at 4-weeks and 8-weeks with UBM injection, but the 8-week animals had a higher

OARSI score than the 4-week animals. To evaluate this further, a 12-week time point could be done to look at long-term therapeutic effects to assess if the benefit of UBM injections is temporal in nature. Multiple injection of UBM (weekly) would also be interested to look at to see if it increases therapeutic potential long-term.

3.6 Figures

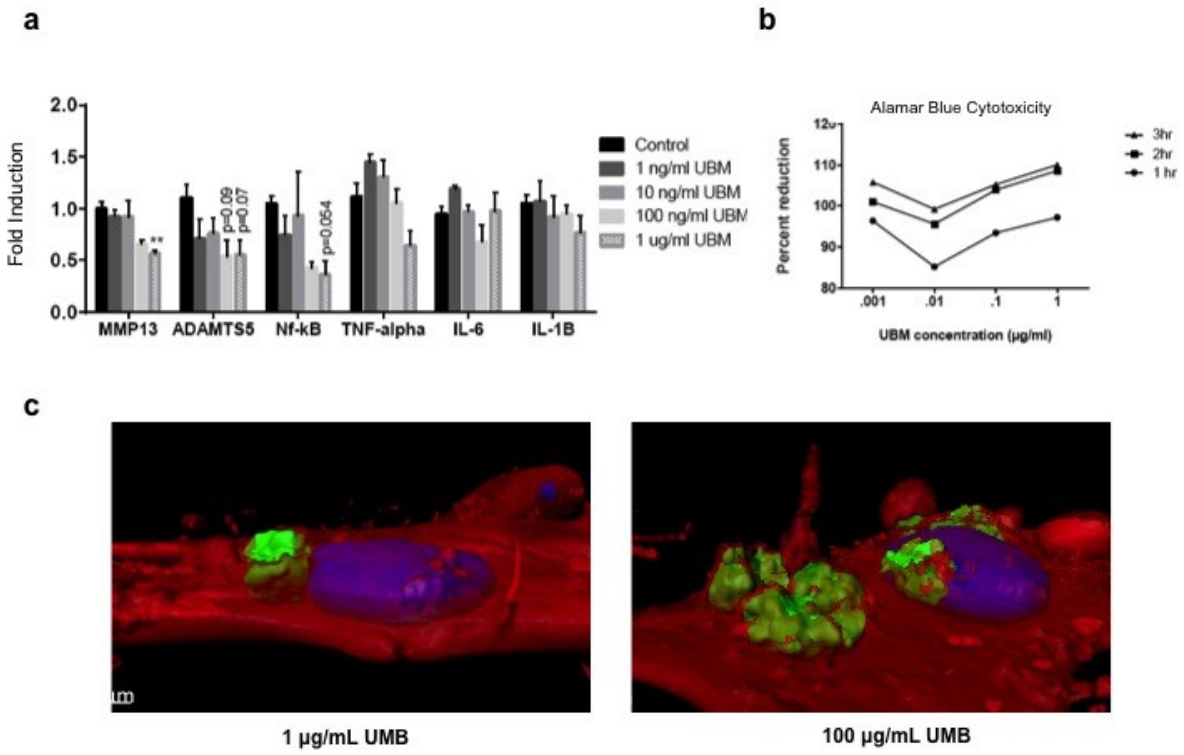

Figure 3.1 UBM decreased inflammatory markers in human primary OA chondrocytes **(a)** Quantification of mRNA expression for MMP13, ADAMTS5, NF-κβ, TNF-alpha IL-6, IL-1β in chondrocytes incubated with Matristem (n=3 per group). **(b)** Alamar Blue Cytotoxicity test for varying concentrations of UMB. **(c)** Confocal imaging of 1ug/ml UBM (left) and 100ug/ml UBM (right) 24 hours after addition into cell culture medium. Red=cell membrane (50% transparency), Blue=nucleus, Green=UBM.

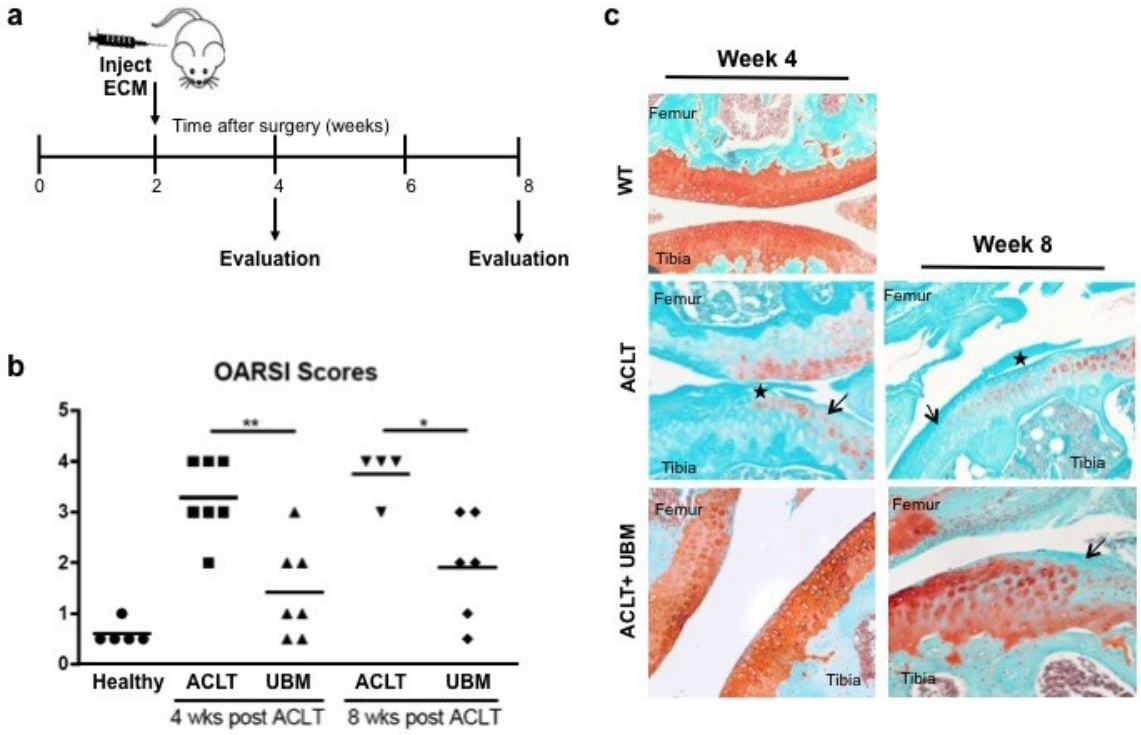

Figure 3.2 UBM treated mice show reduced OA progression by histological analysis
(a) Experimental Schematic of Treatment. C57BL/6 mice undergoing the ACLT of one hind limb to induce OA was injected intra-articular with vehicle (Veh) or 50 mg/ml UBM (10µm-20µm particle size) 2 weeks post-surgery and scarified at 4-week and 8-week time points. **(b)** OARSI scores from the medial tibial plateau of each animal. **(c)** Representative images from each group (N=3 animals per group) with safranin-o staining for proteoglycans.

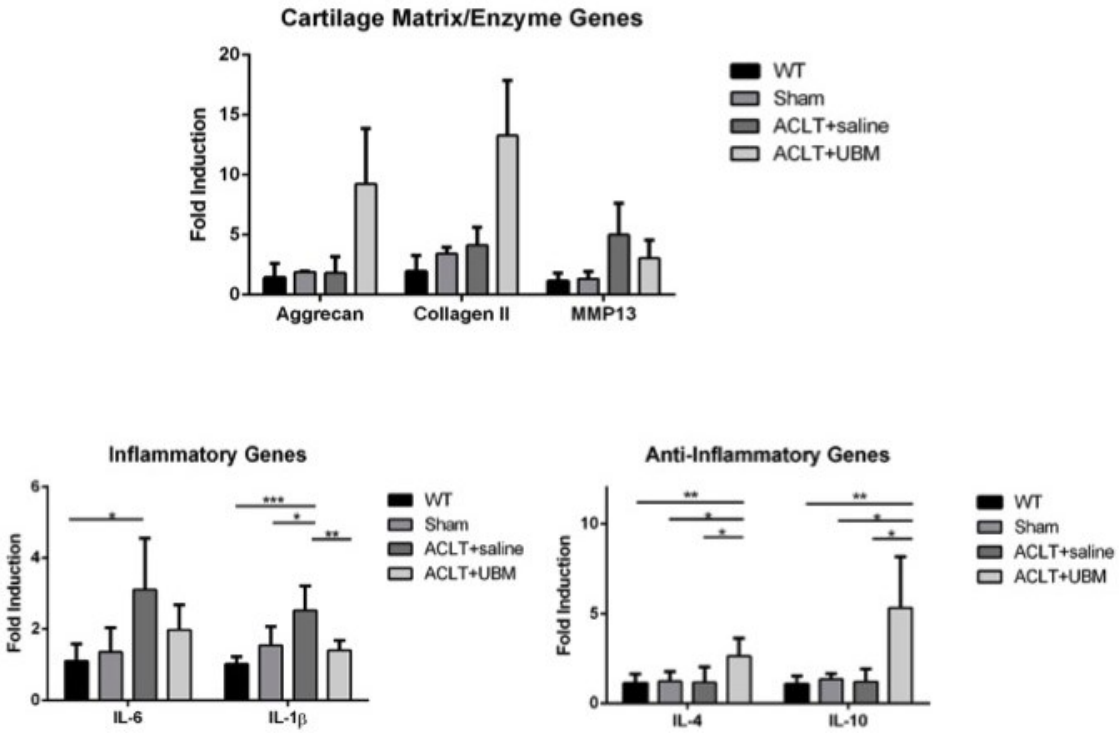

Figure 3.3 UBM treatment Increases Cartilage Matrix and Anti-Inflammatory Genes and Decreases Inflammatory Genes

Mice that underwent the ACLT of one rear limb treated with saline or UBM. Quantification of mRNA expression for cartilage matrix genes (aggrecan, collagen II, MMP13), inflammatory genes (IL-6, IL-1β) and anti-inflammatory genes (IL-4, IL-10) in joints on day 28 after ACLT, n=3 for each group.

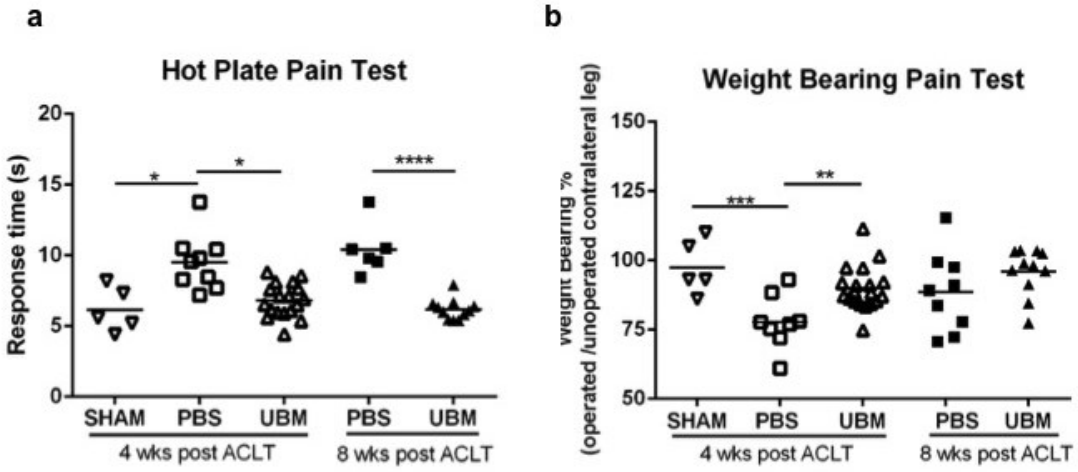

Figure 3.4 UBM treated mice show reduction in OA-related pain
(a) Response time of mice after placement onto a 55°C hotplate 4 weeks and 8 weeks after ACLT surgery for all treatment groups **(b)** The percentage of weight placed on the operated limb versus contralateral control 4 weeks and 8 weeks after ACLT surgery

3.7 References

[1] Badylak, S. F., Freytes, D. O., & Gilbert, T. W. (2009). Extracellular matrix as a biological scaffold material: structure and function. Acta biomaterialia, 5(1), 1-13.

[2] Frantz, C., Stewart, K. M., & Weaver, V. M. (2010). The extracellular matrix at a glance. Journal of cell science, 123(24), 4195-4200.

[3] Benders, K. E., van Weeren, P. R., Badylak, S. F., Saris, D. B., Dhert, W. J., & Malda, J. (2013). Extracellular matrix scaffolds for cartilage and bone regeneration. Trends in biotechnology, 31(3), 169-176.

[4] Alberts, B., Johnson, A., Lewis, J., Raff, M., Roberts, K., & Walter, P. (2002). The extracellular matrix of animals.

[5] Willett, N. J., Thote, T., Lin, A. S., Moran, S., Raji, Y., Sridaran, S., ... & Guldberg, R. E. (2014). Intra-articular injection of micronized dehydrated human amnion/chorion membrane attenuates osteoarthritis development. Arthritis Res Ther, 16(1), R47.

[6] Sasse, K. C., Warner, D., Ward, S. M., Mandeville, W., & Evans, R. (2015). Intestinal Staple Line Reinforcement Using MatriStem. Surgical Science, 6(02), 65.

[7] Brown, B., Lindberg, K., Reing, J., Stolz, D. B., & Badylak, S. F. (2006). The basement membrane component of biologic scaffolds derived from extracellular matrix. Tissue engineering, 12(3), 519-526.

[8] Wolf, M. T., Dearth, C. L., Ranallo, C. A., LoPresti, S. T., Carey, L. E., Daly, K. A., ... & Badylak, S. F. (2014). Macrophage polarization in response to ECM coated polypropylene mesh. Biomaterials, 35(25), 6838-6849.

[9] Lanteri, P. A., Abernathie, B., & Datiashvili, R. (2014). The use of urinary bladder matrix in the treatment of complicated open wounds. Wounds: a compendium of clinical research and practice, 26(7), 189-196.

[10] Sicari, B. M., Rubin, J. P., Dearth, C. L., Wolf, M. T., Ambrosio, F., Boninger, M., ... & Brown, E. H. (2014). An acellular biologic scaffold promotes skeletal muscle formation in mice and humans with volumetric muscle loss. Science translational medicine, 6(234), 234ra58-234ra58.

[11] Wang, M., Sampson, E. R., Jin, H., Li, J., Ke, Q. H., Im, H. J., & Chen, D. (2013). MMP13 is a critical target gene during the progression of osteoarthritis. Arthritis Res Ther, 15(1), R5

[12] Roman-Blas, J. A., & Jimenez, S. A. (2006). NF-κB as a potential therapeutic target in osteoarthritis and rheumatoid arthritis. Osteoarthritis and cartilage, 14(9), 839-848.

[13] Livshits, G., Zhai, G., Hart, D. J., Kato, B. S., Wang, H., Williams, F. M., & Spector, T. D. (2009). Interleukin-6 is a significant predictor of radiographic knee osteoarthritis: The Chingford study. Arthritis & Rheumatism, 60(7), 2037-2045.

[14] Roughley, P. J., & White, R. J. (1980). Age-related changes in the structure of the proteoglycan subunits from human articular cartilage. J Biol Chem, 255(1), 217-224.

[15] Poole, A. R., Kobayashi, M., Yasuda, T., Laverty, S., Mwale, F., Kojima, T., ... & Tchetina, E. (2002). Type II collagen degradation and its regulation in articular cartilage in osteoarthritis. Annals of the rheumatic diseases, 61(suppl 2), ii78-ii81.

[16] Fernandes, J. C., Martel-Pelletier, J., & Pelletier, J. P. (2002). The role of cytokines in osteoarthritis pathophysiology. Biorheology, 39(1, 2), 237-246.

[17] Wojdasiewicz, P., Poniatowski, Ł. A., & Szukiewicz, D. (2014). The role of inflammatory and anti-inflammatory cytokines in the pathogenesis of osteoarthritis. Mediators of inflammation, 2014.

[18] Dieppe, P. A., & Lohmander, L. S. (2005). Pathogenesis and management of pain in osteoarthritis. The Lancet, 365(9463), 965-973.

Chapter 4. Hyaluronic Acid Binding Peptide-Polymer System for Treatment of Osteoarthritis

4.1 Introduction

4.1.1 Synovial Fluid Lubrication

The healthy diarthrotic joint contains a plasma dialysate termed synovial fluid (SF) that is secreted by the synovium to allow for lubrication and passage of nutrients to the cartilage [1]. SF provides boundary film lubrication by the surface interactions of molecules with the articular cartilage that bear load [2] as well as fluid film lubrication where the vicious pressurized fluid between surfaces bears the load [3]. Components of the SF include proteoglycan 4 (lubricin), surface-active phospholipids, and hyaluronic acid (HA) [4] all of which synergistically work together to provide boundary layer lubrication [5]. The focus on the current studies will be on lubrication by HA.

4.1.2 Hyaluronic Acid in the Healthy Joint

HA is a negatively charged [1] linear polysaccharide chain composed of repeating disaccharide units of N-acetyl-glucosamine and glucuronic acid [6] and is the backbone to many proteoglycan complexes [7] such as aggrecan. Given the high molecular weight, HA is responsible for the viscosity of SF and has viscoelastic properties that allow it to serve as a major lubricant to the articulating joint surfaces [7] by allowing surfaces to glide past one another during slow movements and shock absorb during fast movements [6]. Hydration lubrication effect of HA may be due to complex with phosphocholine (PC) groups, present in articular cartilage and the surrounding SF [5]. PC headgroups coat surface-anchored HA creating charged hydration layers that can support high pressures and can be sheared with

less frictional dissipation resulting in low friction between surfaces [5]. HA/PC complexes that are removed by friction are then replenished by HA and PC molecules, produced by chondrocytes and synoviocytes, which permeates the cartilage and synovial cavity [5]. HA may attach to the cartilage surface via entanglements of the linear polysaccharide chain with collagen or another microfibrillar network in the superficial zone [5]. In addition, proteoglycans are retained and anchored to the cartilage surface via HA molecules binding to the CD44 receptor on chondrocytes that also helps facilitate chondrocyte proliferation and functionality [8]. HA also resides in deeper spaces among collagen fibrils and sulfated proteoglycans and thus protects the cartilage by preventing invasion of inflammatory cells into the joint space [8].

4.1.3 Hyaluronic Acid in the Diseased Joint

The lubricating capacity of SF in the osteoarthritic knee joint is compromised due to structural and compositional changes that lead to increased friction, which causes cartilage degradation and abnormal joint movement [9]. Increased levels of pro-inflammatory cytokines such as IL-1 and TNF-alpha, aggrecanases, MMPs, and free radicals disrupt the synthesis of HA [10,8]. Viscosity of SF is also significantly reduced due to proteinases enzymatically cleaving high molecular weight HA into low molecular weight fragments, which are pro-inflammatory [10,8]. Additionally, OA knee joints have reduced lack of binding of HA onto the CD44 receptor, which is correlated with proteoglycan loss on of the cartilage surface [8]. Disruption in the functionality of HA lubrication in the OA joint leads to articular cartilage wear and accelerates disease progression [10].

4.1.4 HA Injection as a Treatment

A well-known treatment that has been used clinically for OA is viscosupplementation in the form of IA injections of hyaluronic acid (HA). These are intended to reduce pain, improve function, and possibly have disease-modifying activity [11]. It has been shown that exogenous HA may promote the production of newly synthesized HA [8]. Cross-linked HA has been developed and used clinically for superior rheological properties, increase retention time in the IA space, and more resistance to free radical degradation [7]. One primary drawback of an HA injection is that it has a short residence time due to degradation by native enzymes [11], lasting about 17 hours for linear HA and 9 days for cross-linked HA [9]. Synvisc®, one commercially available viscosupplement, also does not sufficiently provide sufficient lubrication, as evidenced by its coefficient of friction of 0.119 in contrast to human synovial fluid, which has a coefficient of friction in the range of 0.001 to 0.02 [12,13]. HA also has previously shown to have poor absorption onto OA articular cartilage surfaces, and thus functions poorly as a boundary lubricant once the boundary layer contacts have been lost [2,10]. There exists a need to improve the lubrication ability and retention of HA in viscosupplementation for the goal of better improving OA progression.

4.1.5 HABpep-Polymer System as a Treatment

One possible solution to the limitations of current viscosupplements is anchoring HA onto the load-bearing surface to improve boundary layer lubrication and help retain HA in the IA space for a longer period of time [10] where it can continue to have beneficially biological effects. The HAPpep (HA Binding Peptide)-Polymer system was developed previously in the lab and consists of a bifunctional PEG (thiol-PEG-SGA) core [9]. HABpep was linked via an amine-SGA conjugation reaction to one end of PEG while the thiol end

was functionalized with amine-reactive azlactone [9]. The amine-reactive azlactone functionality was conjugated to a collagen binding peptide so that it can interact with the exposed collagen of OA articular cartilage [9]. A diagram of the HABpep-Polymer system can be seen in **Fig.4.1** [9]. With this system, HABpep binds to HA and tethers it onto the articular cartilage surface.

The ability of the HABpep-polymer system to increase longevity of HA in the IA space was previously evaluated by IA injection into rat joints, where it was shown that use of the system with linear HA increased retention time 12-fold [9]. The goal of the following work is to screen different HABpep and PEG combinations and evaluate the preclinical effectiveness of the HAPpep-polymer system in reducing the progression of OA by modifying disease and providing symptomatic pain relief in a PTOA mouse model.

4.2 Materials and Methods

Surgically Induced OA Mouse Model

ACLT was performed on 10-week old C57BL/6 mice as previously described in **Section 2.2.1**.

IA Injection

Two weeks post surgery, a single 10 µL IA injection of following treatments: PBS (n=6), HA (20mg/mL; n=6), HABP1/Linear PEG (10mg/mL; n=6), HA+HABP1/Linear PEG (n=5), HABP1/Linear PEG (20mg/mL; n=3), HABP2/Linear PEG (50mg/mL; n=3), HABP3/Linear PEG (50mg/mL, n=3), HABP1/8-Arm PEG (50mg/mL, n=3), HABP2/8-Arm PEG (25mg/mL, n=3) was administered to the mice in the operated knee using a 30-guage needle.

Histological evaluation:

Histological evaluation was performed as previously described in **Section 2.2.1**.

Weight Bearing Assessment:

Weight bearing assessment was performed as previously described in **Section 2.2.1**.

Hot Plate Assessment:

Hot Plate Assessment was performed as previously described in **Section 2.2.1**.

Statistical Analysis

Statistical analysis was done with a one-way ANOVA with Holm-Sidak multiple comparison correction in GraphPad Prism Software. $P < 0.05$ was considered significant.

4.3 Results and Discussion

HA Binding Peptide treated mice reduces OA progression by histological analysis

In order to determine the clinical efficacy of use of different HABpep Binding Systems, three different HABpep (HABP1, HABP2, HABP3) and two different PEGs (Linear, 8-arm) were injected IA into ACLT mouse model of PTOA. HABP1 at the low concentration, and HABP1+HA, showed a significant increase in proteoglycan content than ACLT group **(Fig 1a).** The HABP1+HA has a lower average OARSI score than the HABP1 or HA groups individually thus the combination of peptide plus HA is promising **(Fig 1b).** HABP2 alone looked only slightly better than the ACLT group, but combined with 8-ARM

PEG showed significant increase in proteoglycan content **(Fig 1a)** and decrease in OARSI score **(Fig 1b).**

Overall, the use of the HABpep-polymer system was most efficacious on reducing the progressing of OA with HABP2 bound to 8 arm PEG, which is proposed to be due to the increased retention time of HA onto the cartilage surface therefore providing boundary lubrication through interactions and fluid film lubrication by presence in the SF and increase in viscosity. In addition to mechanical functionality, HA molecule itself can have disease modifying activity *in vivo* and has been shown *in vitro* studies to increases proteoglycan content of chondrocytes from rabbit, house, and bovine [8]. It has also been shown that HA can suppress cartilage damage caused by fibronectin fragments which bind and penetrate cartilage and increase MMP levels thus suppressing proteoglycan synthesis [8]. Additionally, HA has also been shown to stimulate synthesis of cartilage matrix components and chondrocyte growth [10].

HA Binding Peptide Reduces OA-Related Pain

Functional pain testing was performed to screen peptides for alleviation of OA-related pain. Mice injected with HABP1 and both linear and 8-arm PEG had significantly decreased latency time when put on a 55°C platform compared to other peptide and control groups **(Fig 4.3a).** Weight bearing pain test however showed that HABP2 had the most even distribution of weight on each hind leg **(Fig.4.23).** HABP1 with linear PEG was not significant most likely due to variability in the group, and HABP2 with 8-arm PEG was also not significant, although it showed a more even distribution in weight than the control groups **(Fig.4.3b).**

Pain relief by HA could be attributed to the effect of HA on nerve impulses and sensitivity [8]. Administration of HA to isolated medial articular nerves has showed decreased nerve activity and movement evoked activity in addition to reducing nerve impulses from an inflamed knee model [8]. The antinociceptive effect of HA was also seen in dose-dependent manner in rats, which may be due to attenuation of prosteoglandin E_2 and bradykinin synthesis [8]. Another way HA can effect pain is by modulating the pharmacology of substance P, a mediator in pain through interactions with excitatory amino acids, prosteoglandins, and nitric oxide [8]. Increasing HA retention through use of the binding peptide could potentially increase binding to neuropeptides, creating a better boundary layer around nocireceptors thus reducing pain [10].

4.4 Conclusions

In vivo screening of different peptides and PEG formulations showed that HABP2 and 8-arm PEG showed to be the most promising HABpep-polymer system that has the ability to best mitigate cartilage degeneration and proteoglycan loss while reducing pain. This therapeutic effect shows disease modifying ability and can be attributed to the increased retention time in the joint that allows for additionally boundary layer lubrication and longer exposure of HA to the chondrocytes increasing proteoglycan secretion. HA could also potentially have disease modifying attributes due to its ability to interact with collagen and chondrocytes and thus modulating inflammatory mediators [14] such as reduction in TNF-alpha, MMP3, and IL-1β as previously seen [8]. Additional lubrication that the system provides may increase binding to neuropeptides and create a boundary around nocireceptors causing a reduction in symptomatic pain.

4.5 Future Directions

This study showed an optimal HApep-polymer system in terms of efficacy in treatment of OA. In the future, studies can be done to determine the appropriate dosing regime, for example multiple doses, of the HA injections as well as looking at long-term effects on OA by having longer time points. Although a retention study was already performed in the rat, it would also be useful to replicate the same study in the mouse model and to further characterize the binding properties and coefficients of the different formations.

4.6Figures

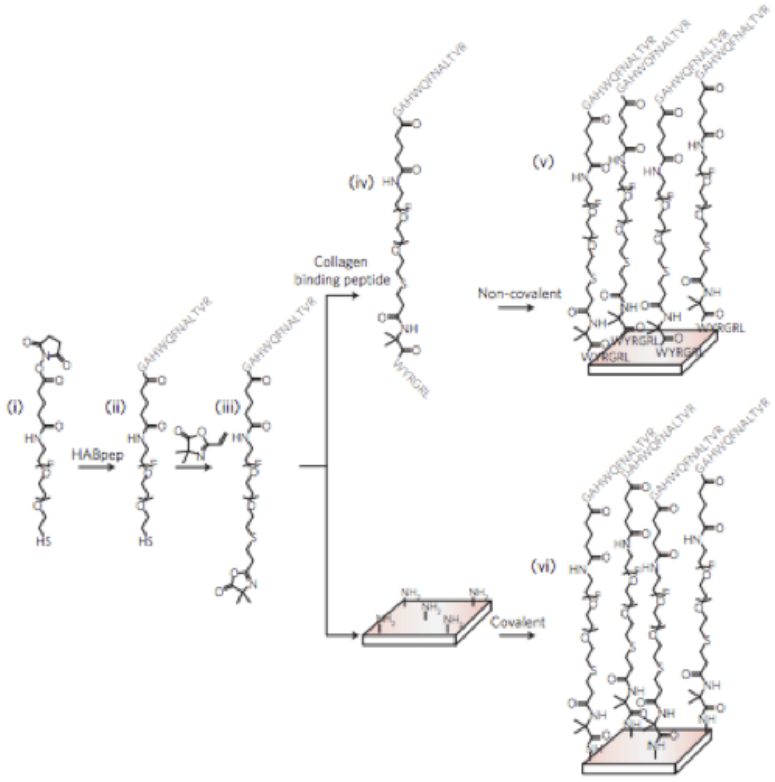

Figure 4.1 Synthesis of HABpep-Polymer Binding system [13]
A diagram of the synthesis of the HABpep-polymer system involving a HA binding peptide, bifunctional PEG linker, functionalization groups, and HA.

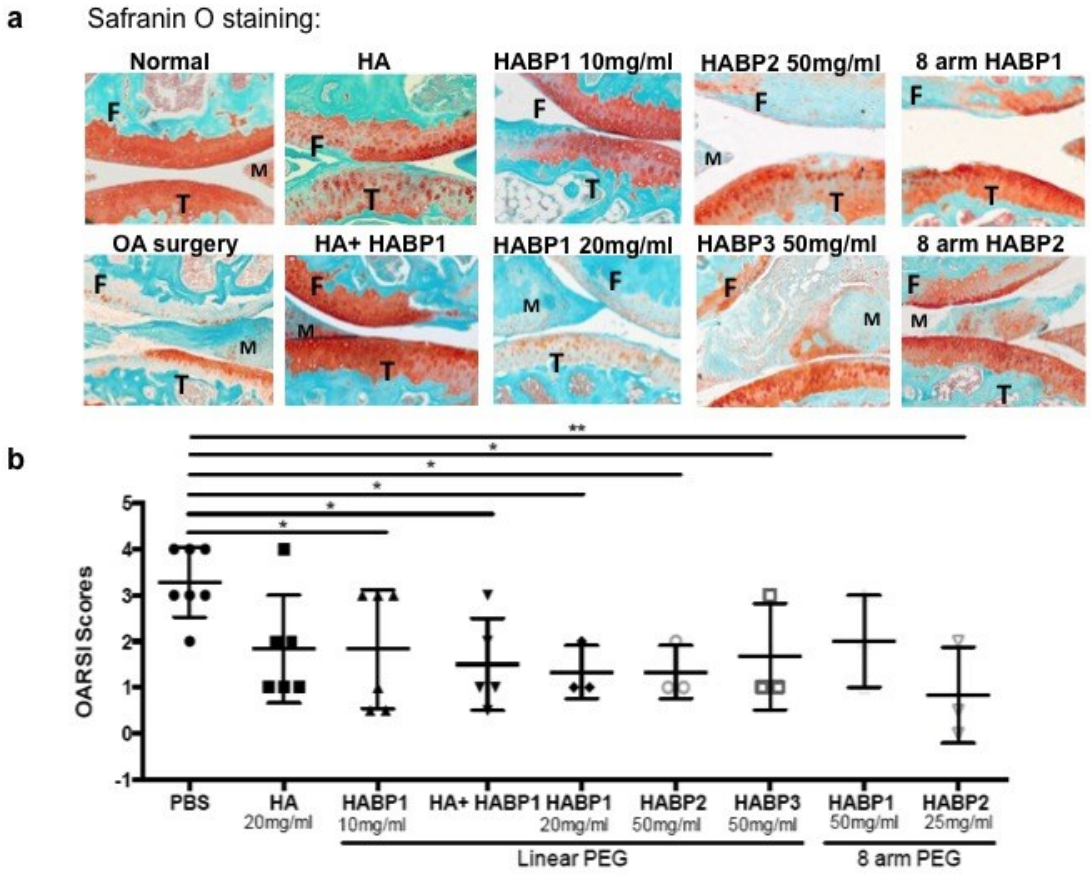

Figure 4.2 HA and Binding Peptide System can Reduce the Progression of OA
(a) Representative images safranin O/methyl green from C57BL/6 mice to evaluate the pathological changes 4 weeks after ACLT. (PBS, n=6; HA 20 mg/ml, n=6; HABP1 10 mg/mL, n=6; HA+HABP1, n=6; HABP1 20 mg/ml, n=3; HABP2 50 mg/ml, n=3; HABP3 50 mg/ml, n=3; HABP1 50 mg/ml, n=3, HABP2 25 mg/ml, n=3) **(b)** OARSI scores from the medial plateau of each animal.

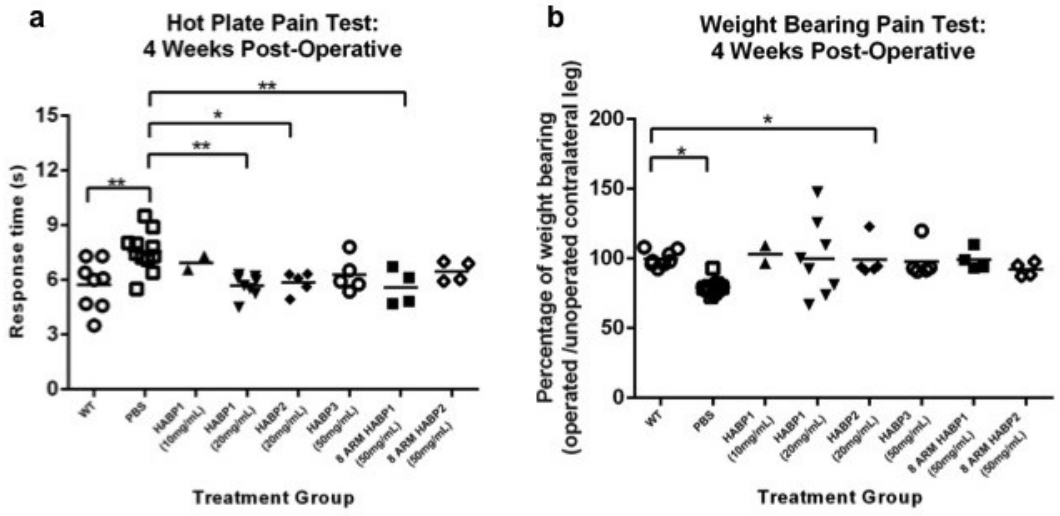

Figure 4.3 HA and Binding Peptide System can Reduce Symptomatic OA-Related Pain **(a)** Response time of mice after placement onto a 55°C hotplate 4 weeks and 8 weeks after ACLT surgery for all treatment groups. **(b)** The percentage of weight placed on the operated limb versus contralateral control 4 weeks and 8 weeks after ACLT surgery.

4.7 References

[1] Chang, D.P., Abu-Lail, N.I., Coles, J.M,, Guilak, F., Jay, G.D., Zauscher, S. (2009). Friction force microscopy of lubricin and hyaluronic acid between hydrophobic and hydrophilic surfaces. *Soft Matter*. 5:3438–3445.

[2] Bosman R. and Schipper D.J. Microscopic Mild Wear in the Boundary Lubrication regime. Laboratory for Surface Technology and Tribology, Faculty of Engineering Technology, University of Twente, P.O. Box 217, NL 7500 AE Enschede, The Netherlands.

[3] San Andrés. L. "Introduction to pump rotordynamics, Part i. Introduction to hydrodynamic lubrication". ("MEEN626 Lubrication Theory Class:Syllabus FALL2006")

[4] Schmidt, T. A., Gastelum, N. S., Nguyen, Q. T., Schumacher, B. L., & Sah, R. L. (2007). Boundary lubrication of articular cartilage: role of synovial fluid constituents. Arthritis & Rheumatism, 56(3), 882-891.

[5] Seror, J., Zhu, L., Goldberg, R., Day, A. J., & Klein, J. (2015). Supramolecular synergy in the boundary lubrication of synovial joints. Nature communications, 6.

[6] Evanich, J. D., Evanich, C. J., Wright, M. B., & Rydlewicz, J. A. (2001). Efficacy of intraarticular hyaluronic acid injections in knee osteoarthritis. Clinical orthopaedics and related research, 390, 173-181.

[7] Creamer, P., Sharif, M., George, E., Meadows, K., Cushnaghan, J., Shinmei, M., & Dieppe, P. (1994). Intra-articular hyaluronic acid in osteoarthritis of the knee: an investigation into mechanisms of action. Osteoarthritis and Cartilage, 2(2), 133-140.

[8] Moreland, L. W. (2003). Intra-articular hyaluronan (hyaluronic acid) and hylans for the treatment of osteoarthritis: mechanisms of action. Arthritis Research and Therapy, 5(2), 54-67.

[9] Singh, A., Corvelli, M., Unterman, S. A., Wepasnick, K. A., McDonnell, P., & Elisseeff, J. H. (2014). Enhanced lubrication on tissue and biomaterial surfaces through peptide-mediated binding of hyaluronic acid. *Nature materials*, *13*(10), 988-995.

[10]Goldberg, V. M., & Goldberg, L. (2010). Intra-articular hyaluronans: The treatment of knee pain in osteoarthritis. *Journal of Pain Research, 3*, 51-56. doi:10.2147/JPR.S4733

[11] Wathier, M., Lakin, B.A., Bansal, P.N., Stoddart, S.S., Synder, B.D., and Grinstaff, M.W. (2013). A large molecular weight polyanion, synthesized via ring-opening metathesis polymerization, as a lubricant for human articular cartilage. *Journal of the American Chemical Society*, 135: 4930-33.

[12] Dedinaite, A. (2012). Biomimetic lubrication. *Soft Matter*, 8:273.

[13] Merkher, Y., A Sivan, S., A Etsion, I., A Maroudas, A., A Halperin, G., A Yosef, A.. A rational human joint friction test using a human cartilage-on-cartilage arrangement, Tribology Letters, Volume 22, Pages 29-36, http://dx.doi.org/10.1007/s11249-006-9069-9

[14] Palmieri, B., Rottigni, V., & Iannitti, T. (2013). Preliminary study of highly cross-linked hyaluronic acid-based combination therapy for management of knee osteoarthritis-related pain. Drug Des Devel Ther, 7, 7-12.

Chapter 5: Conclusion and Future Directions

The work presented in this thesis shows three different therapeutic approaches to the problem of OA, a disease that affects 33.6% of those 65 years of age and older in the United States. A PTOA mouse model was used to evaluate each of these therapies in terms of gene expression, histological evaluation, and behavioral pain testing. Clearance of SCs *in vitro* and *in vivo* by Nutlin-3a mitigates symptomatic pain while modifying disease by generation a pro-chondrogenic environment with reduction of inflammatory and SASP factors resulting in cartilage matrix regeneration. UBM also showed the ability to reduce pro-inflammatory cytokines and hindered the progression of OA and reduced pain *in vivo*. Lastly, the HABpep-polymer system also showed increased proteoglycan production and reduced pain. Although all these treatments were explored separately, the multi-faceted nature of OA calls for a toolbox of treatments in order to treat all aspects of the disease the most efficiently.

It is possible that the correlated outcomes of the three explored approaches show relationship between lubrication, ECM biomaterial, and senescence. ACLT surgery causes accumulation of SCs that is partially from stresses due to mechanical dysfunction. Theoretically HA injections should help to further normalize this mechanical dysfunction by providing load-bearing properties and thus may reduce the stress stimuli causing the DDR and induction of SCs and therefore helping to reduce SC development. ECM injections could also potentially reduce SC development by lowering the cytokine levels as seen *in vitro*. Combinations of the presented treatments could be explored further in the future.

Chapter 6: Curriculum Vitale

S o n a R a t h o d

12 Spring Court Birdsboro, PA 19508 • (610) 306-7057 • sona.rathod21@gmail.com

E D U C A T I O N

Johns Hopkins University — Baltimore, MD
Masters of Science in Biomedical Engineering — May 2016

Drexel University — Philadelphia, PA
Bachelor of Science in Biomedical Engineering — June 2014
A.J. Drexel Scholarship and Dean's List — **Magna Cum Laude: 3.78/4.00**

W O R K E X P E R I E N C E

Translational Tissue Engineering Center, Johns Hopkins University — *Baltimore, MD*
Graduate Student Researcher — *August 2014-May 2016*

- Collaborating with industry/academic experts to revert disease-related aging in the knee joint caused by osteoarthritis
- Conducting animal studies for translation of hyaluronic acid-based injectable for lubrication treatment of osteoarthritis joints
- Determining the utility of de-cellularized matrix biomaterial in regeneration of cartilage tissue in diseased knee joints

Biomaterials Research Group, Drexel University — *Philadelphia, PA*
Senior Design Capstone Project — *September 2013-June 2014*

- Developed a novel viscosupplement from biomimetic aggrecan for use in osteoarthritic knee joints
- Designed biomimetic aggrecan to have lubrication and viscoelastic properties to mimic human synovial fluid
- Performed rheometry and friction testing of viscosupplement prototype on cartilage model system and created a theoretical model in MATLAB to predict the frictional and viscoelastic properties of the prototype

Vascular Kinetics Laboratory, Drexel University — *Philadelphia, PA*
Research Assistant — *September 2013-June 2014*

- Performing assays to measure reactive oxygen species production of bovine endothelial cells
- Measuring the fluorescence of endothelial cells after treatment conditions and analyzing data with ImageJ software
- Conducting proliferation assays to measure endothelial cell growth after treatment conditions

Danaher Corporation: Imaging Sciences International, Gendex, Dexis *Hatfield, PA*
Advanced Development Engineer *March 2013-September 2013*

- Worked with cross-functional team of 9-members to develop test procedures to meet German tomography standards
- Developed a GUI to model joint friction of an articulating arm using MATLAB for use in design iterations
- Conducted a mathematical analysis of image quality of competitive intraoral sensors for benchmark studies
- Tested intraoral sensors for electrical and mechanical failure and generated reports of the results
- Conducted pediatric phantom head positioning on 3D computer tomography instruments

The Children's Hospital of Philadelphia (CHOP) *Philadelphia, PA*
Product Development Engineer, Critical Care/Anesthesiology *June 2011-October 2011*

- Generated a review of endotracheal intubation and included recommendations for device improvements
- Acquired stress and strain data during CPR compressions of pediatric thoracic cavity and common objects such as a soccer ball
- Created a stimulation in MATLAB of CPR compressions based on the properties of the object undergoing compression
- Presented findings to CHOP and Drexel faculty at STAR (Students Tackling Advanced Research) Research Symposium

DESIGN PROJECTS

Novel Bone Cement Formulation to Reduce Aseptic Loosening: Proposed an idea to incorporate a biodegradable hydrogel made of PEG/PLA block copolymers conjugated to PNIPAAm into PMMA bone cement to reduce the aseptic loosening caused from exothermic reaction

Dual Sensor Heat Stroke Monitor: Developed an idea to create a monitor to prevent heat stroke by sensing both temperature and heart rate; proposed a possible circuit design as well as wireless components to improve ease of use; included analysis of human factors

Femoral Implant with Improved Osseointegration*:* Created 3D model on Creo Parametric for hip implant that increases osseointegration and decreases stress shielding; included assembly, working drawings, dimensioning, tolerances, and bill of materials

Coronary Heart Disease Software-Business Plan: Created a business plan for a software-based product for patients and doctors to help prevent onset of coronary heart disease; business plan

included marketing plan, analysis of competitive environment, financial predictions, and a strategic operational and management plan

Career Skill Development Social Entrepreneurship Project: Developed an idea for a non-profit social entrepreneurship business to teach developing community career development skills that increase confidence and facilitate them to create opportunity

L E A D E R S H I P

Global Engineering Innovation: *Team Leader* *July 2015-Present*

- Leading a team of 7 students to develop affordable technologies to address healthcare issues in developing nations

Biomedical Engineering Innovation Program: *Teaching Assistant* *May 2014-Present*

- Teaching graduate students lab techniques and engaging students in group discussions of biomedical technology

Johns Hopkins Technology Venture: *Team Leader* *June 2015-December 2015*

- Organized a team to assess the commercialization potential of a novel orthopedic medical device

U.S. Dream Academy Philadelphia: *Service Coordinator* *September 2012–June 2014*

- Mentored 7 at-risk youth every week improving their motivation and academic performance in math and science

Alpha Kappa Psi Professional Business Fraternity: *Service Chair* *December 2011–June 2014*

- Established relationships with 10 community service centers for bi-weekly volunteer trips for organization members

S K I L L S

Software: CREO Parametric, AutoCAD, Microsoft Office Suite/Project, MATLAB, GraphPad Prism, Maple, ImageJ

Laboratory: drug delivery systems, drug development, biomaterials, mechanical testing, cell culture, biocompatibility testing

Business: business canvas model, business plans, competitive market analysis, technical writing, engineering documentation

P U B L I C A T I O N S

Rahman, T., Nishisaki, A., Fiadjoe, J. E., **Rathod, S**., Kritzer, D., & Deutsch, E. S. (2015). Evaluating the Mechanics of Laryngoscopy: A Review. Journal of Clinical Engineering, 40(1), 43-50.